

Detection of autoantibodies specific for inflammation-associated proteins in COVID-19 patients

Lugar, Marija

Master's thesis / Diplomski rad

2022

Degree Grantor / Ustanova koja je dodijelila akademski / stručni stupanj: **University of Zagreb, Faculty of Science / Sveučilište u Zagrebu, Prirodoslovno-matematički fakultet**

Permanent link / Trajna poveznica: <https://um.nsk.hr/um:nbn:hr:217:579521>

Rights / Prava: [In copyright](#) / [Zaštićeno autorskim pravom.](#)

Download date / Datum preuzimanja: **2024-11-21**



Repository / Repozitorij:

[Repository of the Faculty of Science - University of Zagreb](#)



University of Zagreb
Faculty of Science
Department of Biology

Marija Lugar

**Detection of autoantibodies specific for
inflammation-associated proteins in
COVID-19 patients**

Master thesis

Zagreb, 2022.

Sveučilište u Zagrebu
Prirodoslovno-matematički fakultet
Biološki odsjek

Marija Lugar

**Detekcija autoantitijela specifičnih za
proteine upale kod oboljelih od bolesti
COVID-19**

Diplomski rad

Zagreb, 2022.

This graduation thesis was conducted at the Bonifacio laboratory group of the Center for Regenerative Therapies Dresden, Cluster of Excellence, TU Dresden, under the supervision of Prof. Ezio Bonifacio, PhD and cosupervision of Assoc. Prof. Petra Korać, PhD. The thesis was submitted to the evaluation of the Department of Biology at the Faculty of Science, University of Zagreb to obtain the title of Master of Molecular Biology (mag.biol.mol.).

Acknowledgments

First and foremost, I would like to express my sincere gratitude to Prof. Ezio Bonifacio for introducing me to the world of antibodies and trusting me with such an interesting and exciting thesis project. It has been a true privilege to learn from you.

I cannot begin to express my thanks to my dear mentors Dr. Anne Eugster and Denise Müller, who guided me through this thesis and taught me many tips and tricks. I will forever be grateful for your unwavering support and your kindness.

A special thank you goes to Prof. Petra Korać for her co-supervision. Thank you for always being helpful and understanding.

I would like to thank the rest of my “Bonis” for all the lunches, coffees, and beers we shared. Thank you for your support and advice, especially for cheering me up on those not-so-great days when things were not going as planned.

Lastly, I would like to thank my friends for making sure I didn't forget to have fun during this journey. I want to thank my friends Ivona and Maša for always believing in me and being there when I needed them. A special thank you goes to my friends Katarina, Lucija, and Vida for making the past 7 “uni” years a fond and unforgettable experience that only the four of us will truly know to appreciate.

Finally, I want to thank my parents, Barbi and André for their unconditional love and support.

BASIC DOCUMENTATION CARD

University of Zagreb
Faculty of Science
Department of Biology

Master thesis

Detection of autoantibodies specific for inflammation-associated proteins in COVID-19 patients

Marija Lugar

Rooseveltovej trg 6, 10000 Zagreb, Croatia

Coronavirus disease 2019 (COVID-19) manifests a variety of symptoms: from being asymptomatic or mild in most of the infected individuals, to causing more severe and even life-threatening conditions in about 20% of the patients. As an effector of the immune system and a hallmark of autoimmunity, autoantibodies are hypothesized to play a role in the pathogenesis of COVID-19 and pose a risk for a severe disease outcome. Hence, this thesis aimed to detect and investigate the prevalence of autoantibodies in sera from COVID-19 patients. Thereby, 100 hospitalized COVID-19 patients of different disease severity (42 moderate and 58 severe/critical) and 41 SARS-CoV-2 seronegative healthy blood donors were tested for autoantibodies specific for different inflammation-associated proteins (interferon (IFN), complement, and DDX helicases) by the luciferase immunoprecipitation system (LIPS) assay. The results show a high prevalence of autoantibodies measured in hospitalized COVID-19 patients (51%) in contrast to the control group (12.2%). However, only 8% of the patients had high and/or intermediate titers (IFN autoantibodies), whereas, in the remaining autoantibody-positive patients only low autoantibody titers were detected. Autoantibodies specific for complement proteins and DDX helicases were detected only in low titers. Interestingly, contrary to previous reports, no association with disease severity, sex, or age was observed for IFN autoantibodies. Overall, the findings suggest that from the measured autoantibodies, IFN autoantibodies could be a relevant prognostic marker in COVID-19, specifically for COVID-19 patients that require hospitalization. The findings emphasize the importance of a wider investigation of autoantibodies in COVID-19.

Keywords: SARS-CoV-2, complement proteins, DEAD-box helicases, cytokines, cross-reactivity, molecular mimicry, LIPS assay

(59 pages, 11 figures, 9 tables, 57 references, original in English)

The thesis is deposited in Central Biological Library.

Mentor: Prof. Ezio Bonifacio, PhD

Co-mentor: Assoc. Prof. Petra Korać, PhD

Reviewers: Assoc. Prof. Petra Korać, PhD
Prof. Zorana Grubić; PhD
Prof. Domagoj Đikić, PhD

Thesis accepted: September 8th, 2022

TEMELJNA DOKUMENTACIJSKA KARTICA

Sveučilište u Zagrebu
Prirodoslovno-matematički fakultet
Biološki odsjek

Diplomski rad

Detekcija autoantitijela specifičnih za proteine upale kod oboljelih od COVID-19

Marija Lugar

Rooseveltov trg 6, 10000 Zagreb, Hrvatska

Bolest COVID-19 (od eng. *coronavirus disease 2019*) uključuje širok spektar simptoma: većina zaraženih pojedinaca nemaju simptome ili imaju blage simptome, dok se kod otprilike 20% slučajeva manifestira teški ili kritični oblik bolesti. Pretpostavlja se da autoantitijela, kao jedan od aktera imunskog sustava te obilježje autoimunih bolesti, imaju ulogu u patogenezi bolesti COVID-19 te da predstavljaju rizik za razvoj težeg oblika bolesti. Glavni cilj ovog rada bio je detektirati autoantitijela kod bolesnika oboljelih od bolesti COVID-19. Kako bi se ispitala prisutnost autoantitijela specifičnih za proteine upale (interferona (IFN), proteina komplementa te helikaze DEAD-box), uzorci 100 bolesnika oboljelih od bolesti COVID-19, od toga 42 s umjerenim i 58 s težim/kritičnim oblikom bolesti, te 41 uzorak SARS-CoV-2 seronegativnih zdravih donora krvi testirani su na autoantitijela imunoprecipitacijskim testom luciferaze (LIPS, od eng. *luciferaze immunoprecipitation system*). Rezultati ukazuju na visoku prevalenciju autoantitijela kod hospitaliziranih bolesnika oboljelih od bolesti COVID-19 (51%) u odnosu na kontrolnu skupinu (12.2%). Međutim, tek 8% pacijenata imalo je srednji ili visoki titar autoantitijela, isključivo specifičnih za IFN, dok je kod ostalih pacijenata pozitivnih na autoantitijela uočen tek nizak titar autoantitijela. Autoantitijela specifična za ostale testirane antigene sustava komplementa i helikaza DEAD-box detektirana su u vrlo niskom titru. Zanimljivo je da suprotno rezultatima prijašnjih studija, u ovom radu nije uočena povezanost IFN autoantitijela s dobi, spolom ili težinom bolesti. Rezultati ukazuju da od testiranih autoantitijela, jedino ona specifična za interferone mogu biti potencijalni marker bolesti COVID-19, posebice za hospitalizirane pacijente. Ovi rezultati pridodaju važnosti šireg istraživanja autoantitijela kod oboljelih od bolesti COVID-19.

Ključne riječi: SARS-CoV-2, proteini komplementa, helikaze DEAD-box, citokini, krosreaktivnost, molekularna mimikrija, LIPS esej
(59 stranica, 11 slika, 9 tablica, 57 literaturnih navoda, jezik izvornika: engleski)
Rad je pohranjen u Središnjoj biološkoj knjižnici.

Mentor: prof. dr. sc. Ezio Bonifacio
Komentor: Izv. prof. dr. sc. Petra Korać

Ocjenitelji: izv. prof. dr. sc. Petra Korać
prof. dr. sc. Zorana Grubić
prof. dr. sc. Domagoj Đikić

Rad prihvaćen: 08.09.2022

Abbreviations

ACE2 - angiotensin-converting enzyme 2

APCs - antigen-presenting cells

C1r - complement C1r subcomponent

C1s - complement C1s subcomponent

C2 - complement C2

CDS - coding DNA sequence

CFB - complement factor B

CFD - complement factor D

COVID-19 - coronavirus disease 2019

DDX3X - DEAD box protein 3, X-chromosomal

DDX58 - DEAD box protein 58

E - Envelope protein

ECMO - extracorporeal membrane oxygenation

HLA - human leukocyte antigen molecules

IFN - interferons

IFN-I - type I interferon

LIPS - Luciferase Immunoprecipitation System

M - Membrane protein

MERS-CoV - Middle East respiratory syndrome coronavirus

NLuc - nanoluciferase

NP - nucleoprotein

NSP - non-structural protein

NSP13 - non-structural protein 5, helicase

NSP5 - non-structural protein 5, or chymotrypsin-like protease, or 3C-like protease

RBD - receptor-binding domain

S - Spike protein

S1 - S1 domain

S2 - S2 domain

SARS-CoV - severe acute respiratory syndrome coronavirus

SARS-CoV-2 - severe acute respiratory syndrome coronavirus 2

SP-IL6 - signal peptide of IL6

SpO₂ - oxygen saturation

WHO - World Health Organization

Table of contents

1. Introduction	1
1.1. COVID-19	1
1.2. SARS-CoV-2	3
1.3. Immune response to SARS-CoV-2	5
1.3.1. Antibody response against SARS-CoV-2	5
1.4. Cross-reactive SARS-CoV-2 antibodies	7
1.4.1. Complement and DDX helicases as autoantigens	8
1.5. Autoantibodies in COVID-19	10
2. Objectives	12
3. Materials and methods	13
3.1. Materials	13
3.1.1. Serum samples	13
3.2. Methods	15
3.2.1. Restriction cloning of recombinant nanoluciferase-tagged antigens	15
3.2.1.1. Polymerase chain reaction (PCR)	15
3.2.1.2. Restriction digest	17
3.2.1.3. Ligation and transformation	19
3.2.1.4. Preparation of plasmid DNA	20
3.2.2. Expression of recombinant antigens	21
3.2.3. Luciferase Immunoprecipitation System (LIPS) assay	22
3.2.3.1. LIPS protocol	23
3.2.4. Statistical analysis	24
4. Results	25
4.1. Production of nanoluciferase-tagged antigens	25
4.2. Establishment of standards for the LIPS assay	27
4.3. Detection of SARS-CoV-2 RBD, S2, and NP antibodies	29
4.4. Autoantibodies specific for inflammation-associated proteins	30
4.4.1. IFN autoantibodies	31
4.4.2. Complement and DDX autoantibodies	33
4.5. Detection of SARS-CoV-2 NSP antibodies	36
5. Discussion	37
6. Conclusion	40
7. References	41
8. Curriculum vitae	48
9. Supplement	49

1. Introduction

1.1. COVID-19

A novel RNA virus from the family of *Coronaviridae* emerged in late 2019 in Wuhan, China (*Disease outbreak news*, WHO, 2020). Severe acute respiratory syndrome coronavirus 2 (SARS-CoV-2) causes the coronavirus disease 2019 (COVID-19) which has quickly taken precedence over all other public health concerns. Two and a half years after the first outbreak of COVID-19, the pandemic is still in full swing with over 500 million confirmed cases and over 6 million deaths reported to the World Health Organization (WHO) up to July 20th, 2022 (*WHO Coronavirus (COVID-19) Dashboard*, WHO, 2022).

Like the other pandemic coronaviruses, severe acute respiratory syndrome coronavirus (SARS-CoV) and Middle East respiratory syndrome coronavirus (MERS-CoV), SARS-CoV-2 is transmitted through respiratory droplets and spreads rapidly. However, SARS-CoV-2 has a much higher transmission rate than SARS-CoV and MERS-CoV because many cases of infection are asymptomatic or very mild and remain undiagnosed (Abdelrahman et al., 2020). Most of the cases are asymptomatic or mild with common symptoms like fever, dry cough, fatigue, loss of taste and smell, diarrhea, headache, and muscle pain. However, some patients develop severe pneumonia with low oxygen levels ($SpO_2 < 94\%$), experiencing dyspnoea (shortness of breath) and chest pain. In such severe cases, patients need oxygen therapy. Oxygen therapy is given in form of supplemental oxygenation or high-flow oxygenation, depending on the severity of the patient's condition. Supplemental oxygen is administered through a nasal cannula or a non-rebreather mask, whereas, for high-flow oxygenation, mechanical ventilation is needed. In the case of ventilation, positive pressure can be delivered through a mask (non-invasive ventilation) or a tube (intubation). All patients that require ventilation are hospitalized in the intensive care unit (ICU). Rarely, patients end up being in a critical state when respiratory failure, multiple organ failure, and/or sepsis occur. Critical patients need extracorporeal membrane oxygenation (ECMO) and may need other organ support as well (*Clinical Spectrum - COVID-19 Treatment Guidelines*, NIH, 2022, Wiersinga et al., 2020) (Table 1). Lastly, there are the so-called "long COVID" patients with symptoms persisting for weeks or months after the onset of the infection. Long after being infected, these patients are usually reporting symptoms of autonomic dysfunction, dyspnoea, and extreme fatigue, and some may also be experiencing neurocognitive difficulties (Sudre et al., 2021).

In summary, patients show very heterogeneous responses to the virus in severity and duration of symptoms. Apart from age, sex, and comorbidities like obesity, diabetes, chronic kidney disease, chronic lung disease, hypertension, immunosuppression, malignancies, and others (Kaeuffer et al., 2020, Sudre et al., 2021), various immunological features also pose a major risk for a severe disease

outcome. Particularly, inborn errors of immunity and autoantibodies intensively investigated for their contributions to the pathogenesis of COVID-19 have been associated with disease severity (Bastard et al., 2020, Hadjadj et al., 2020, Wang et al., 2021,).

Table 1. COVID-19 categorized by disease severity according to NIH (*Clinical Spectrum - COVID-19 Treatment Guidelines*, NIH, 2022).

COVID-19 category	Frequency (Stokes et al., 2020)	Symptoms	Hospitalization	Oxygen treatment
Asymptomatic	79%	no symptoms	no	no
Mild		common symptoms: fever, cough, sore throat, fatigue, headache, diarrhea, loss of taste and smell, muscle pain	no	no
Moderate	21%	lower respiratory disease during clinical assessment or imaging, with SpO ₂ ≥94% (mild pneumonia)	yes, normal ward	no
Severe		lower respiratory disease with SpO ₂ ≤94% (severe pneumonia)	yes, normal ward or ICU	supplemental oxygen or or high-flow oxygenation
Critical		respiratory failure, multiple organ system failure, sepsis	yes, ICU	ECMO

1.2. SARS-CoV-2

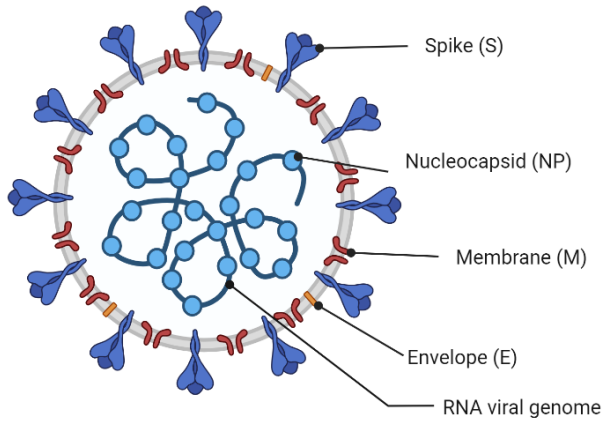
SARS-CoV-2 belongs to *Coronaviridae*, a family of large, enveloped, and single-stranded RNA viruses. Its genome is a positive-sense RNA with a 5'-cap and a 3'-polyadenylated tail making it suitable for translation by the host's translation machinery. At the 5'-end two open reading frames (ORF), ORF1a and ORF1ab start, encoding two polyproteins, PP1a and PP1ab, respectively. These polyproteins are proteolytically processed into 16 non-structural proteins (NSP1-16) (Naqvi et al., 2020).

Four types of structural proteins are encoded at the 3'-end: Spike protein (S), Membrane protein (M), Envelope protein (E), and nucleoprotein (NP). NP binds viral RNA and packs it into a capsid which is protected within an envelope. The envelope consists of three different structural proteins: S, M, and E. Proteins M and E build the membrane structure of the envelope while the transmembrane S protein in form of homotrimers projects from the envelope surface and mediates virus entry into host cells (Satarker & Nampoothiri, 2020). The projections of S protein on the surface are a distinct feature of coronaviruses. They are thought to resemble the form of a crown under the electron microscope, hence their name (*lat. corona* = crown) (Li, 2016). The S protein monomer has two functional domains: S1 and S2. The receptor binding domain (RBD) through which S protein interacts with angiotensin-converting enzyme 2 (ACE2) receptors lies within the S1 domain, while the S2 domain mediates virus-host membrane fusion (Huang et al., 2020).

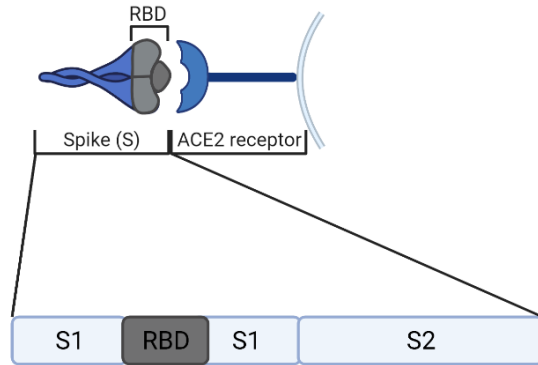
Non-structural proteins (NSP) are a group of various enzymes and transcription factors facilitating viral replication and transcription. The RNA-dependent RNA polymerase (NSP12) with its cofactors, NSP7 and NSP8, and helicase (NSP13) forms the transcriptional and replicational machinery of the virus. NSP14 is a 3'-5' exoribonuclease with proofreading activity ensuring the stability of the viral genome. The two cysteine proteases, NSP3 (papain-like protease) and NSP5 (chymotrypsin-like protease, also referred to as 3C-like protease) cleave the polyproteins into non-structural proteins. At 3'-end there are six other ORFs encoding accessory proteins whose roles are yet to be discovered (Figure 1) (Wang et al., 2020).

After transmission, SARS-CoV-2 binds to the ACE2 receptors on the epithelial cells in the host's body. ACE2 receptors are expressed in the colon, kidney, heart, gallbladder, cornea, upper respiratory tract, and lungs (Li et al., 2020). The virus enters the cells via endocytosis or membrane fusion. Inside the cell, its RNA is released and translated by the host's translation machinery. Newly synthesized non-structural proteins replicate the viral genome. Simultaneously, structural proteins are synthesized. Ultimately, the RNA is packed into enveloped virions that are released from the cells by exocytosis. These virions spread through the bloodstream and the neighboring cells causing an infection (Malone et al., 2022).

A. SARS-CoV-2 structure



B. Spike (S) protein



C. SARS-CoV-2 genome

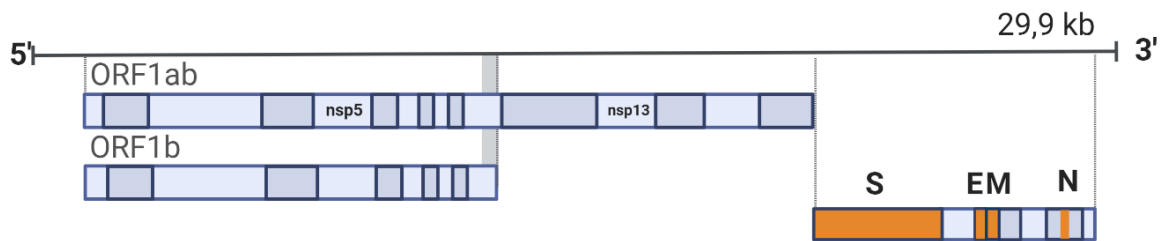


Figure 1. Schematic of SARS-CoV-2 virus. A. Schematic structure of SARS-CoV-2. B. Schematic structure of Spike protein and binding to ACE2 receptor. C. Schematic SARS-CoV-2 genome. The figure was based on data from NCBI, GenBank entry NC_045512.2, and created with BioRender using the template “Human Coronavirus Structure”.

1.3. Immune response to SARS-CoV-2

Upon first contact with a new pathogen, innate immunity is immediately activated as the first line of defense. In the early phase of the infection, inflammatory factors are released along with mannose-binding lectin, chemokines, naturally occurring glycan-binding antibodies, NK and $\gamma\delta$ -T cells, the proteins of the complement system, and interferons. They help stimulate antigen-presenting cells (APCs) such as dendritic cells, macrophages, and epithelial cells. APCs break down the viral antigens into small peptides that are then presented within human leukocyte antigen molecules (HLA) on the APCs surface. HLA I activates the cytotoxic T cells that then directly attack the infected cells, whereas HLA II activates helper T cells which release cytokines and chemokines to stimulate cytotoxic T cells and B cells (Boechat et al., 2021). When overstimulated, helper T cells produce excessive amounts of pro-inflammatory cytokines (IFN- α , IFN- γ , IL-1 β , IL-6, IL-12, IL-18, IL-33, TNF- α , TGF β , etc.) and chemokines (CCL2, CCL3, CCL5, CXCL8, CXCL9, CXCL10, etc.) which causes a physiological phenomenon known as the cytokine storm (Hu et al., 2021). High cytokine levels are observed in severe and critical patients, whose immune system is overstimulated and is chaotically attacking the body, including healthy tissue, which can result in multiple organ failure, septic shock, and even death (Shcherbak et al., 2021). SARS-CoV-2 can also bind to the lower parts of the respiratory tract including the alveoli. In the alveoli, type II alveolar cells produce the surfactant - a molecule that maintains the surface tension of the alveoli wall enabling effective gas exchange in the lungs. In severe cases, SARS-CoV-2 attacks type II alveolar cells triggering cell apoptosis, subsequently disturbing the pulmonary homeostasis and causing lung edema, hypoxia, and dyspnoea (Calkovska et al., 2021).

1.3.1. Antibody response against SARS-CoV-2

Adaptive immunity, including B-cell mediated humoral and T-cell mediated immunity, is a key antiviral defense that helps to eliminate the invading virus in a specific way and develops a long-term immunologic memory against it. Once stimulated by viral peptides presented on APCs, B cells can proliferate and differentiate into antibody-producing plasma cells or memory B cells, ultimately producing large amounts of virus-specific antibodies (Röltgen & Boyd, 2021). During a SARS-CoV-2 infection, antibodies to the structural and non-structural proteins are produced (Jiang et al., 2020, Shrock et al., 2020). IgM and IgG antibodies are rapidly produced and can already be detected in serum a week post-symptom onset (Figure 2). IgG titers are more stable than IgM titers and can be detected in sera from recovered or vaccinated individuals for months after the infection (Cervia et al., 2022, Secchi et al., 2020). The gold standard in serological testing for SARS-CoV-2 is the detection of antibodies specific for highly antigenic structural proteins: S and NP (Liu et al., 2020). Apart from the cytotoxic lymphocytes (mainly CD8+ T cells), neutralizing antibodies are a major effector of adaptive immunity that has the potential to neutralize the virus and help cytotoxic lymphocytes to eliminate it. SARS-CoV-

2 neutralizing antibodies recognize the S protein and bind to the RBD and N-terminal domain of the S1 region or S2 region, thus blocking the binding to the ACE2 receptors on the host's cells and ultimately impairing viral entry (Xiaojie et al., 2020). In comparison, the non-structural proteins are less antigenic and antibodies to these proteins are rare (Jiang et al., 2020, Matyuskina et al., 2022). Having many highly neutralizing epitopes, the S protein is critical for virus neutralization and constitutes the main component of most vaccines against SARS-CoV-2 (Martínez-Flores et al., 2021). Therefore, in the thus vaccinated individuals, only antibodies against S can be detected, whereas in the infected convalescent individuals both S and NP antibodies can be detected.

Time course of antibody response in COVID-19

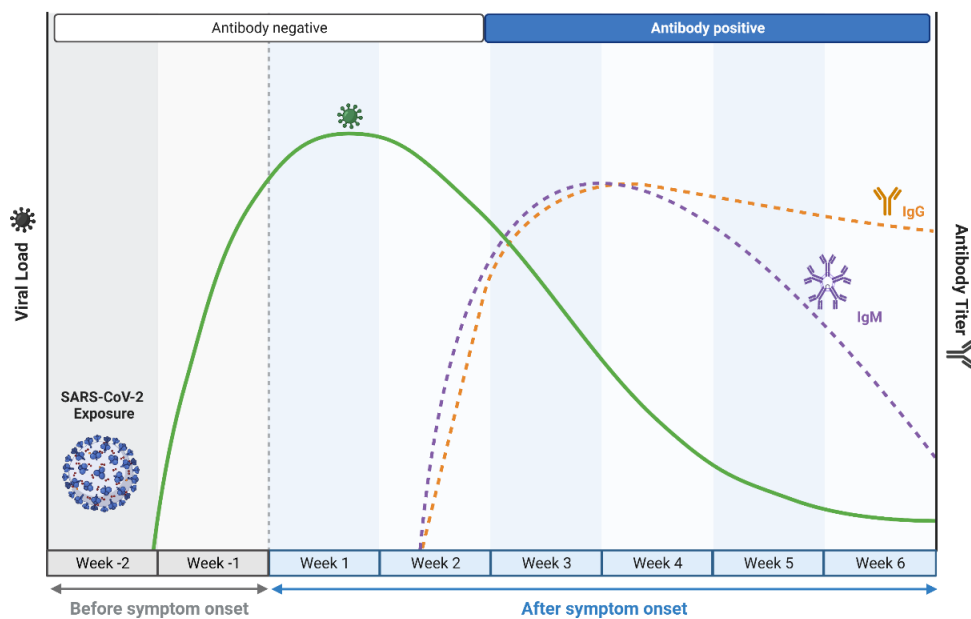


Figure 2. Time course of antibody response in COVID-19. Created in Biorender using a template “Time Course of COVID-19 Infection and Test Positivity”.

1.4. Cross-reactive SARS-CoV-2 antibodies

SARS-CoV-2 proteins share strong sequence homology with proteins of other human coronaviruses such as SARS-CoV, MERS, HKU1, OC43, 229E, and NL63, especially between structural proteins. This results in a three-dimensional structural similarity of epitopes between the antigens. Therefore, an antibody originally raised against a specific antigen may cross-react and bind to another structurally similar antigen, such as a protein of another coronavirus (Bates et al., 2020, Grobden et al., 2021).

Not only can such cross-reactivity occur between proteins of different viruses, but such phenomenon may also occur between viral and human proteins that share strong structural and/or linear sequence homology. A pair of unrelated proteins of similar molecular design is called a mimicked pair. According to the molecular mimicry hypothesis, an infection can offset the response in the host against its own antigens (autoantigens) that are similar to the pathogen proteins. Such an event leads to the breakdown of self-tolerance, activation of autoreactive T cells, and production of autoantibodies where the pathogen-directed immune response is misled towards self-antigens (Maoz-Segal & Andrade, 2015). A large number of autoimmune diseases potentially associated with infections due to molecular mimicry between the pathogen and human proteins were described (Cuisick et al., 2012): e.g. enteric viruses and type 1 diabetes (Baum et al., 1995), Enterobacteriaceae and rheumatoid arthritis (Aoki, 1999), and herpesviruses and systemic lupus erythematosus (SLE) (McClain et al., 2005). Noteworthy, some studies have reported cross-reactivity of the SARS-CoV-2 antibodies, mainly those against NP and S protein, with proteins that are known autoantigens like the insulin and GAD-65 in type 1 diabetes (Vojdani et al., 2021), cytokeratin-18 in chronic obstructive pulmonary disease (Kuo et al., 2010, Matyuskina et al., 2022), and M2 in autoimmune encephalomyelitis (Lebar et al., 1989, Vojdani et al., 2021). The mechanism of cross-reactivity for the mentioned examples of cross-reactive SARS-CoV-2 antibodies is unknown.

Several research groups have mapped mimicked pairs of SARS-CoV-2 and human proteins (Lasso et al., 2021, McGill et al., 2022, Squeglia et al., 2020). Lasso et al. annotated 158 human proteins structurally mimicked by coronaviruses. Among those, the non-structural SARS-COV-2 proteins NSP5 and NSP13 are of interest for this thesis because they are structural mimics of several inflammation-associated proteins: proteins of the complement system (CFB, CFD, C1s, C1r, and C2) and DDX helicases (DDX3X and DDX58) (Table 2) (Lasso et al., 2021). Antibodies targeting proteins of the complement system and DDX helicases are of particular interest as they have been described in some autoimmune diseases and carcinomas (Trendelenburg, 2021, Welberry et al., 2020). Furthermore, McGill et al. mapped 346 structural mimicked pairs using a different strategy. Among them were also some proteins of the complement system (CFB and C1s) and DDX58 as structural homologs of SARS-CoV-2 proteins (McGill et al., 2022). Another study has also mapped various DDX helicase proteins as

structural mimics of the SARS-CoV-2 NSP13 protein (Squegla et al., 2020). It must be noted that the mentioned studies used different strategies for mapping structurally similar proteins which resulted in a discrepancy between the reported pairs: e.g., Lasso et al. found the CFB to be structurally similar to the NSP5 protein, whereas McGill et al. mapped it as a mimicked pair of the S protein. Furthermore, Squegla et al. found structural similarities of NSP13 with 11 different DDX helicase proteins including the DDX3X, but not with the DDX58. Nonetheless, a part of this thesis will focus on the findings of Lasso et al. and investigate the prevalence of complement and DDX helicase-specific autoantibodies as well as the presence of antibodies that bind to their mimicked viral protein pairs, proteins NSP5 and NSP13.

Table 2. SRAS-CoV-2 structural mimicked protein pairs of complement and DDX helicase proteins mapped by Lasso et al. (Lasso et al., 2021).

Mimicked viral protein		Mimicked human protein		
SARS-CoV-2 protein	Homology domain	Human protein	UniProt ID	Full-length protein size
NSP13	260-582 aa	DEAD box protein 58 (DDX58)	O95786	925 aa
		DEAD box protein 3, X-chromosomal (DDX3X)	O00571	662 aa
NSP5	1-301 aa (full-length)	Complement C2 (C2)	P06681	752 aa
		Complement C1r subcomponent (C1r)	P00736	705 aa
		Complement C1s subcomponent (C1s)	P09871	688 aa
		Complement factor B (CFB)	P00751	764 aa
		Complement factor D (CFD)	P00746	253 aa

1.4.1. Complement and DDX helicases as autoantigens

The complement system dynamically surveys the immune system and comprises about 50 proteins and fragments, including serum proteins and receptor proteins. The complement system is activated by antibodies (classical pathway), pattern recognition receptors such as mannose-binding lectin and ficolins (the lectin pathway), and by spontaneous hydrolysis of the C3 component (alternative pathway) that functions as a positive-feedback loop. Activation of complement pathways triggers a protease cascade by which proteins are cleaved into fragments and then those fragments bind to form new complexes, forming convertase complexes, and ultimately forming a membrane-attack complex

(MAC) that can directly lyse the pathogens or infected cells. Some complement proteins also facilitate phagocytosis via opsonization and some even act as potent cytokines that can enhance the inflammatory response and attract macrophages and neutrophils (Stoermer & Morrison, 2011). Altogether, these proteins have an important role in the immune defense against invading pathogens, including viruses. Therefore, autoantibodies targeting complement proteins could potentially affect the function of these proteins which could ultimately result in dysregulation of the immune response against the invading pathogen.

The DDX helicases are a group of cellular RNA helicases that partake in RNA metabolism, including RNA-RNA and RNA-protein remodeling. During an infection, these helicases are involved in viral replication, which they can affect positively or negatively. It is believed that in SARS-CoV-2 infection these proteins have a pro-viral role in a way that the virus can hijack the DDX helicases and use them to facilitate its replication. Dysregulation of these proteins was correlated with oncogenesis, inflammation, viral replication, and immune response (Squeglia et al, 2020). Although the exact role of these proteins in viral infections is still unclear, there is enough evidence to suspect that the autoantibodies targeting DDX helicases could potentially influence the viral infection.

Complement autoantibodies have been associated with some autoimmune diseases such as systemic lupus erythematosus (Trendelenburg, 2021) and neuromyelitis optica spectrum disorder (Uzonyi et al., 2021). In SLE patients, the most commonly detected autoantibodies are anti-C3, anti-C4, anti-C1q, anti-CFP, and anti-CFH, but other less frequent ones such as anti-C1s were also detected (Pradhan et al., 2021, Trendelenburg, 2021). Unlike the complement autoantibodies, less is known about the DDX-helicase autoantibodies. A study found DDX3X autoantibodies in sera from hepatocellular carcinoma patients and suspected them to play a role in carcinogenesis (Welberry et al., 2020). I found no other reports of DDX helicase autoantibodies.

1.5. Autoantibodies in COVID-19

In some patients, the SARS-CoV-2 infection is suspected to disrupt the self-tolerance of the immune system, subsequently setting off an autoimmune response through cross-reactivity with the host's antigens. COVID-19 resembles autoimmune diseases in its clinical outcomes, as well as in aspects of the immune response and pathogenic mechanisms (Liu et al., 2021). Autoantibodies, a hallmark of autoimmunity, were reported in COVID-19 patients (Bastard et al., 2020, Wallukat et al., 2021, Wang et al., 2021). The hypothesis is that COVID-19 can induce new autoantibodies or increase the number of existing ones in genetically susceptible patients. These autoantibodies are likely directed against proteins involved in the immune response (such as complement proteins, cytokines, and chemokines) or organ-specific antigens, hence, they can directly attack the tissues and organs expressing the target antigen or indirectly cause damage by forming immunocomplexes with autoantigens. Furthermore, this theory could also explain the late onset of symptoms and their persistence in long-COVID patients because it takes weeks for autoantibodies to develop (Khamsi, 2021). Wang et al. performed an extensive study on 194 COVID-19 patients, screening their sera for antibodies against a wide spectrum of antigens. They found a clear increase in reactive autoantibodies in patients compared to the uninfected controls, directed mainly against cytokines, chemokines, complement components, and cell surface proteins. Also, the tests of patients' sera obtained longitudinally confirmed both pre-existing and newly induced antibodies (Wang et al., 2021). Bastard et al. detected autoantibodies against IFN α 2 and/or IFN ω in 13.7% of the severe COVID-19 patients during the acute phase. These autoantibodies are known to neutralize their target (its corresponding type of IFN) thus impairing binding to IFN receptors. Interestingly, the presence of these autoantibodies was specific to the patients with severe pneumonia, while none were detected in mild/asymptomatic patients. In this case, the authors speculate these antibodies to precede COVID-19 rather than being induced during infection; moreover, they presume them to be a key factor in driving the course of illness toward severe and life-threatening outcomes (Bastard et al., 2020). Therefore, a part of this thesis will focus on detecting IFN autoantibodies in COVID-19 patients. Deficiency of the type I interferon (IFN-I) pathway can arise due to inherited mutations in genes that encode proteins of type I IFN pathway, or due to type I IFN-specific neutralizing autoantibodies. Both result in decreased levels of functional IFN-I proteins. Interferons (IFN) are a type of cytokines that "interfere" with a viral infection, mainly inhibiting viral replication in host cells, and helping the body to eliminate the virus. The IFN-I family consists of 13 IFN- α subtypes, IFN- β , IFN- ω , IFN- κ , and IFN- ϵ . A repressed IFN-I response leads to uncontrolled viral replication and invasion of host cells enhancing the severity of the disease (McNab et al., 2015). Other autoantibodies such as autoantibodies against G-protein coupled receptors (predominantly against β 2-adrenoreceptor and muscarine M2-receptor) were found in COVID-19 patients. The authors suspect them to play a role in the development of cardiac and neurological symptoms, which are also observed among COVID-19 patients (Wallukat et al., 2021).

To date, multiple studies have confirmed the significance of autoantibodies in COVID-19 patients supporting the autoimmunity hypothesis (Bastard et al., 2020, Wallukat et al., 2021, Wang et al., 2021). Scientists and clinicians have recognized the volume and importance of autoantibodies in COVID-19 patients and are focusing their efforts on organizing studies that could clarify the pathological mechanisms involved. The longitudinal follow-up is of great importance in these studies. It is important to understand whether autoimmunity appears before the onset of the infection, during the acute phase, or after being infected, and whether it correlates with the severity of the symptoms. In general, it is of great importance to investigate the prevalence of autoantibodies in COVID-19 to better understand the contribution of autoimmunity in the pathogenesis of the disease. Autoantibodies as a hallmark of autoimmunity have the potential to be effectors and/or biomarkers of COVID-19, thus of great help to clinicians to monitor the disease progression and help them to decide which of the medications routinely used to treat autoimmune diseases might also be useful in the treatment of COVID-19.

2. Objectives

This thesis aims to investigate the prevalence and titer of autoantibodies specific for inflammation-associated proteins in sera from COVID-19 patients, specifically, autoantibodies specific for IFN-I (IFN α 1, IFN α 8, IFN α 17, and IFN ω 1), proteins of the complement system (C2, C1r, C1s, CFD, and CFB) and DEAD-box helicases (DDX3X and DDX58). This thesis will also investigate a potential association of the detected autoantibodies with the severity of the disease.

The specific technical aims of this thesis were to establish the LIPS assay standard for autoantigens C2, C1s, C1r, CFD, CFB, DDX3X, and DDX58, and SARS-CoV-2 antigens NSP5 and NSP13.

3. Materials and methods

3.1. Materials

3.1.1. Serum samples

All procedures performed involving human participants were in accordance with the ethical standards of the institutional and/or national research committee and with the 1964 Helsinki Declaration and its later amendments. Informed written consent was obtained from patients and donors included in the study. Ethical approval was obtained from the Technical University of Dresden, Germany.

For the assessment of autoantibody profiles in COVID-19 patients, sera from COVID-19 patients (N=100) sampled from April 6th, 2020 to April 26th, 2021 were obtained from BioBank Desden (BBD), Germany. All COVID-19 patients included in the study were hospitalized at the University Hospital Carl Gustav Carus in Dresden and were confirmed to be SARS-CoV-2 positive by a real-time polymerase chain reaction (RT-PCR) test and/or had symptoms suggestive of COVID-19. They were categorized by the severity of the disease as moderate (N=42) or severe/critical (N=58). The moderate patients were hospitalized in the normal ward and didn't receive oxygen therapy. On the other hand, patients hospitalized in the intensive care unit that received oxygen therapy were categorized as severe/critical. Of the 58 severe/critical cases, 55 were intubated, while the remaining three cases were either not ventilated or had non-invasive ventilation. Almost half of them (N=26) also received ECMO (Figure 3).

As controls, sera from healthy blood donors (N=100) were obtained from the Red Cross, Dresden, Germany. Although the aim was to have pre-pandemic sera as controls, sera collected in May 2021 were available and obtained. Some of these donors are presumed to have already been infected by SARS-CoV-2 and/or have been vaccinated at the time of collection. To form a SARS-CoV-2 seronegative control group, the samples were tested for SARS-COV-2 RBD, S2, and NP antibodies by LIPS assay as previously described (Hippich et al., 2021). In their previous study, Hippich et al. defined the cutoff values for NP, RBD, and S2 at 13 AU, 0.9 AU, and 3 AU, respectively. The same cutoff values were adopted in this thesis to determine the respective antibody-positivity of the samples. Stringent criteria of triple-negativity for all three types of antibodies were applied, i.e. samples that tested negative for all three types of SARS-CoV-2 antibodies were selected as SARS-CoV-2 seronegative healthy controls for the analysis of autoantibodies and NSP antibodies.

All serum samples were stored at -20 °C.

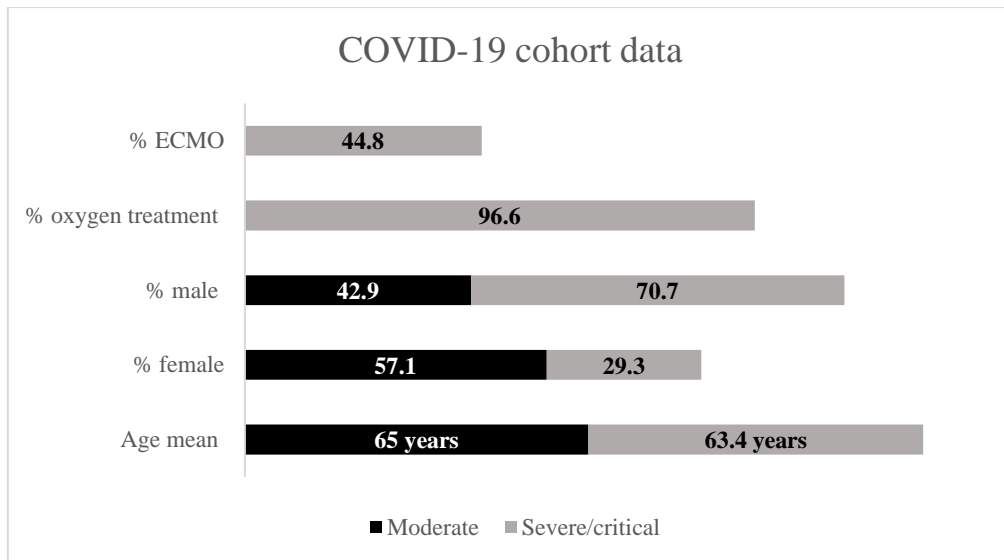


Figure 3. Baseline characteristics of patients infected with COVID-19 (N=100) categorized by the severity of the disease as moderate (N=42) or severe/critical (N=58). All of the severe/critical patients received oxygen therapy and 44.8% received extracorporeal membrane oxygenation (ECMO), whereas, patients categorized as moderate did not receive any oxygen treatment. Age and sex distribution is also shown.

3.2. Methods

3.2.1. Restriction cloning of recombinant nanoluciferase-tagged antigens

I used restriction cloning to obtain plasmids encoding recombinant nanoluciferase-tagged antigens for human proteins C1r, C1s, C2, CFB, CFD, DDX3X, DDX58, and SARS-CoV-2 NSP5 and NSP13.

3.2.1.1. Polymerase chain reaction (PCR)

To obtain inserts suitable for restriction cloning, I performed a polymerase chain reaction (PCR) using a set of 5' and 3' coding DNA sequence (CDS) specific primers with the restriction site used for cloning. For human constructs C1s, C2, CFB, CFD, DDX3X, and DDX58, I used universal human cDNA or human cDNA isolated from the liver or peripheral blood mononuclear cells (PBMCs) as a DNA template in the PCR. For cloning of the SARS-CoV-2 antigens NSP5 and NSP13 aa 206-582, I used CDS sequences synthesized by Eurofins, Germany. I performed the PCR reaction using the primers and DNA templates listed in Table 3. For the PCR I mixed approx. 50 ng of the template DNA, 10 µl of 5x PrimeSTAR Buffer (Takara), 4 µl of 10 mM dNTPs (Takara), 1 µl of 10 µM 5' primer, and 1 µl of 10 µM 3' primer, 0.5 µl of PrimeSTAR HS DNA Polymerase (Takara), and 32.5 µl of DEPC-treated H₂O (Thermo Scientific) in a final volume of 50 µl. I used a PCR cycling protocol of 30 cycles of denaturation at 98 °C for 10 s, annealing at the adjusted temperature for 5 s, and elongation at 72 °C for an adjusted time according to Table 3. The final elongation was at 72 °C for 10 min with storage at 4 °C.

For the cloning of the C1r antigen, the CDS of the full-length C1r already flanked with the restriction sites was synthesized by Genewiz, i.e. the synthesized sequence was directly used for restriction digest reaction.

Table 3. List of primers for restriction cloning of nanoluciferase-tagged antigens and corresponding DNA templates, annealing temperature (Ta), and elongation time used in the polymerase chain reaction (PCR). The restriction site within the primer sequence is in red. F – forward primer or 5’ primer, R – reverse primer or 3’ primer, PBMC - peripheral blood mononuclear cells.

Primer name	F/R	Primer sequence (5’ – 3’)	Ta	Elongation time	DNA template
NSP5_F	F	GGCGGGATCCATGAGTGGTTTTAGAAAAAT	45 °C	1 min	synthesised
NSP5_R	R	GATCAACGGGGCCGCTAATAATAATTGGAAAGTAA CACCTGAGC			
NSP13_F	F	GGCGTGGATCCATGGAGTTTTCTAGCAATGTTGC	50 °C	1min	synthesized
NSP13_R	R	GATCAACGGGGCCGCTAATAATAAATAAAGGTCTC TATCAGACA			
C2_F	F	GGCAGGATCCATGGGCCACTGATGGTTCTT	51 °C	3 min	Universal cDNA
C2_R	R	TCGCCAGCGGGCCGCTAATAATAACTAGAGGGGTAA AAAATTCAG			
C1s_F	F	GGTACTCGAGATGTGGTGCATTGTCCTGTTT	58 °C	3 min	liver cDNA
C1s_R	R	TCGCCAGCGGGCCGCTAATAATAATTAGTCCTCAGG GGGGGTGCT			
CFB_F	F	GGTATCTAGAATGGGGAGCAATCTCAGC	51 °C	3 min	liver cDNA
CFB_R	R	TCGCCAGCGGGCCGCTAATAATAATTATAGAAAACC CAAATCCTC			
CFD_F	F	GGTAGATATCATGCACAGCTGGGAGCGCCTG	62 °C	1 min	PBMC cDNA
CFD_R	R	GGTATCTAGATAATAATAACTAGGCCAGGACGCTG TCGAT			
DDX3X_F	F	GGTAGGATCCATGAGTCATGTGGCAGTGGAA	58 °C	3 min	universal cDNA
DDX3X_R	R	TCGCCAGCGGGCCGCTAATAATAATCAGTTACCCCA CCAGTCAAC			
DDX58_F	F	GGTACTCGAGATGACCACCGAGCAGCGACGC	58 °C	3 min	universal cDNA
DDX58_R	R	TCGCCAGCGGGCCGCTAATAATCATTGGACATTCT GCTGG			

I analyzed the quantity and size of the amplified PCR fragments on 1% agarose gel. I prepared the gel in TBE buffer (0.13 M Tris, 45 mM boric acid, 2.5 mM EDTA, pH 7.6) and added EtBr for visualization of the DNA. I always performed the electrophoresis in TBE buffer at 100 V for a maximum of 1 hour. I visualized the samples under a UV lamp. If more than one band was seen on the gel, I ran the remaining volume of the PCR reaction on a 1% agarose gel and visualized it under a UV lamp to excise the band of the correct size from the gel. I purified the excised DNA by using the QIAquick® Gel Extraction Kit (Qiagen). Otherwise, if only one band was seen on the gel, I directly purified the PCR reaction by using the QIAquick® PCR Purification Kit (Qiagen). Finally, I visualized the purified fragments on 1% agarose gel to estimate their quantity by comparing the bands of the samples to bands of the GeneRuler 1 kb DNA Ladder (Thermo Scientific).

3.2.1.2. Restriction digest

I used a commercially available mammalian expression vector pCMV6-AC-IRES-GFP (Origene, MD, USA) as backbone in cloning of the NLuc-tagged antigens (Figure 4). The signal peptide IL-6 (SP-IL6) for enhanced protein secretion and the Nanoluciferase reporter (NLuc) (Promega) for detection during the luciferase assay (LIPS) were inserted.

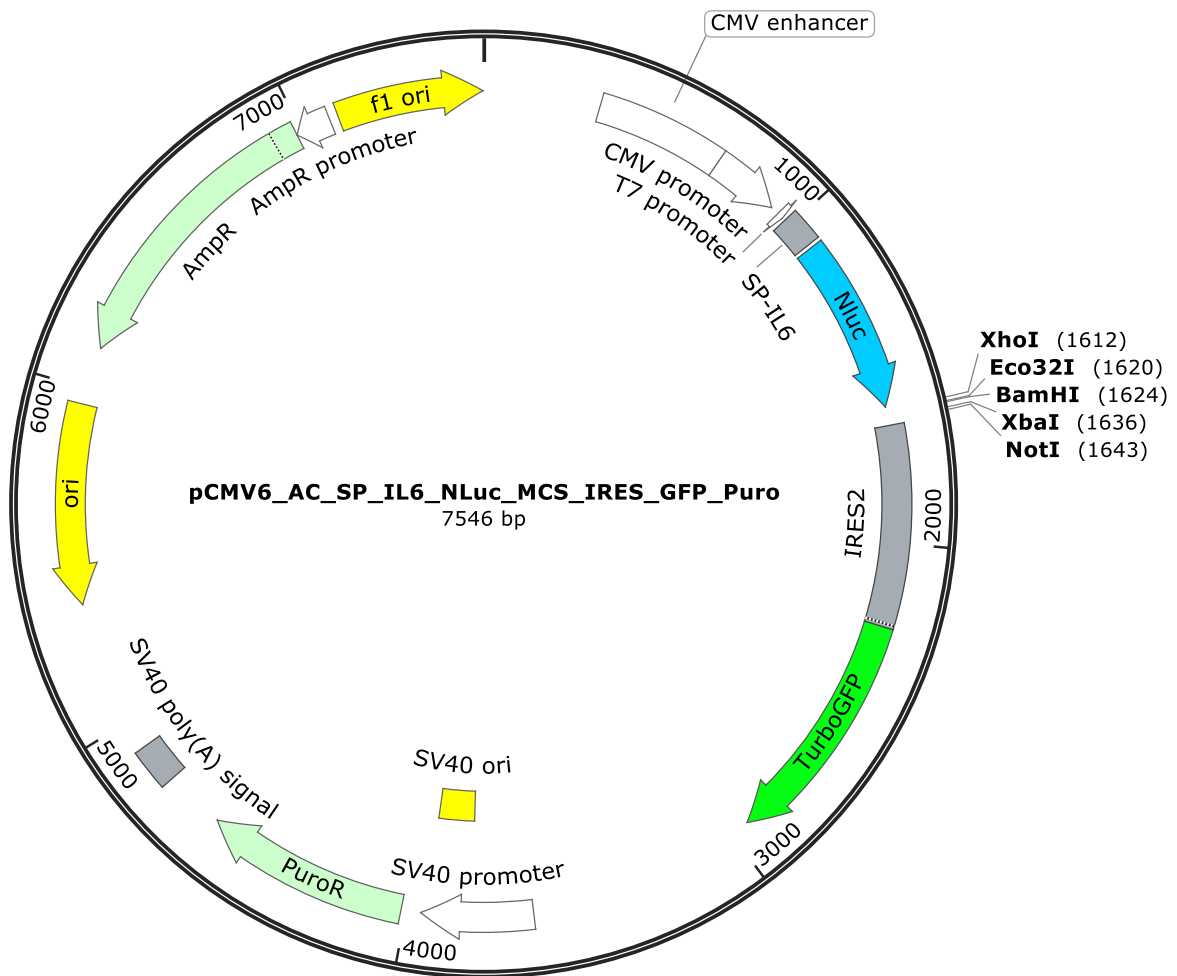


Figure 4. Vector map of the plasmid pCMV6-AC-IRES-GFP-Puro (Origene, MD, USA) used as the backbone in cloning. Under the control of the CMV promoter (pCMV) is the open reading frame (ORF) that includes the coding DNA sequences (CDS) encoding the signal peptide of IL6 (SP-IL6), nanoluciferase (NLuc) followed by the multiple cloning site (MCS) that is used to insert the genes of interest. The GFP is encoded after the internal ribosomal binding site (IRES2) on the plasmid which allows for it to be transcribed independently from the inserted gene of interest. The vector contains the ampicillin and puromycin resistance gene (ampR, puroR) as selective markers.

I used a pair of restriction enzymes to digest the purified PCR fragments and the C1r CDS synthesized DNA (Table 4). I used the same pair of enzymes to digest the target vector as well. To ensure optimal activity of the restriction enzyme, I digested the fragment and vector DNA with each restriction enzyme of the pair separately as described in the following. I mixed approximately 1 ug of fragment or vector DNA with 2 μ l of the restriction enzyme, 4 μ l of the 10x buffer, and distilled water up to a final volume of 40 μ l. The reaction was incubated for two hours at 37 $^{\circ}$ C. To prepare the DNA for the second digest reaction, I precipitated the DNA. I added 60 μ l of distilled water and 70 μ l of isopropanol to the reaction and the samples were centrifuged for 6 min at 13000 rpm. I discarded the supernatant, added 100 μ l of 70% ethanol, and centrifuged it for 5 min at 13000 rpm. To dry the pellet,

I placed the samples into an Eppendorf Vacufuge Plus vacuum concentrator (Eppendorf) for 20 min at 45 °C. I resuspended the DNA in 2 µl of the second restriction enzyme, 4 µl of the enzyme's corresponding buffer, and distilled water up to a final volume of 40 µl. The reaction was incubated for two hours at 37 °C. Finally, I purified the insert DNA using the QIAquick® PCR Purification Kit (Qiagen). I ran the vector digest reaction on a 1% agarose gel and visualized it under a UV lamp. I excised the band corresponding to the size of the vector backbone from the gel and purified it using the QIAquick® Gel Extraction Kit (Qiagen). I ran the purified insert and backbone DNA on a 1% agarose gel to determine the approximate quantity of the DNA.

Table 4. The list of restriction enzymes and buffers used in the digest reaction.

Insert fragment	Restriction enzyme #1	Buffer #1	Restriction enzyme #2	Buffer #2
Nsp5	BamHI	BamHI-Lsp1109I Buffer (10X) (Thermo Scientific)	NotI	Buffer O (10x) (Thermo Scientific)
Nsp13 aa 206-582	BamHI	BamHI-Lsp1109I Buffer (10X) (Thermo Scientific)	NotI	Buffer O (10x) (Thermo Scientific)
C2	BamHI	BamHI-Lsp1109I Buffer (10X) (Thermo Scientific)	NotI	Buffer O (10x) (Thermo Scientific)
C1r	Eco32I	Buffer R (10x) (Thermo Scientific)	NotI	Buffer O (10x) (Thermo Scientific)
C1s	XhoI	Buffer R (10x) (Thermo Scientific)	NotI	Buffer O (10x) (Thermo Scientific)
CFB	XbaI	Buffer Tango (10x) (Thermo Scientific)	NotI	Buffer O (10x) (Thermo Scientific)
CFD	Eco32I	Buffer R (10x) (Thermo Scientific)	XbaI	Buffer Tango (10x) (Thermo Scientific)
DDX3X	BamHI	BamHI-Lsp1109I Buffer (10X) (Thermo Scientific)	NotI	Buffer O (10x) (Thermo Scientific)
DDX58	XhoI	Buffer R (10x) (Thermo Scientific)	NotI	Buffer O (10x) (Thermo Scientific)

3.2.1.3. Ligation and transformation

I ligated the digested inserts and vectors using the T4 DNA ligase (Promega). I set up the ligation reaction using 100 ng of purified vector DNA, 50 ng of purified insert DNA, 1 µl of 10x buffer, and distilled water up to a final volume of 10 µl. The reaction was incubated overnight (max. 18 h) at 16 °C. I transformed chemically competent E. coli JM109 cells by adding 5 µl of the ligation reaction

to 50 μ l of the cell suspension. The cells were first incubated on ice for 20 min, heat-shocked for 45 sec at 42 °C, and placed on ice for an additional 5 min. Afterward, I added 900 μ l of cold SOC medium (B9020S, NewEngland BioLabs) to the cells. The samples were incubated at 37 °C for one hour with shaking at 900 rpm. Finally, I plated the cells on LB agar plates containing ampicillin (100 μ g/mL) and incubated them overnight at 37 °C.

3.2.1.4. Preparation of plasmid DNA

The following day, I picked single colonies and cultured them in 1 ml of LB-Amp medium overnight at 37 °C with shaking at 900 rpm. The next day, I isolated the plasmid DNA by mini preparation using the QIAprep® Spin Miniprep Kit (Qiagen). I measured the concentration of the isolated DNA using the NanoPhotometer Implen (Implen, Germany). To confirm the presence of the insert in the plasmid, I digested the isolated DNA with a restriction enzyme that has at least one restriction site within the insert and at least one restriction site within the plasmid backbone (Table 5). I used 500 ng of plasmid DNA and mixed it with 1 μ l of the restriction enzyme, 1 μ l of the enzyme's 10x buffer, and filled up distilled water to a final volume of 10 μ l. The reaction was incubated for one hour at 37 °C. I ran 5 μ l of the restriction reaction on 1% agarose gel and visualized it under a UV lamp. If the correct number and size of the bands were seen, the plasmid DNA was sequenced at Eurofins, Germany using the Sanger method for final confirmation. I analyzed the sequencing results using CLC Main Workbench 8.1 Software. Finally, cultures with correct plasmids were grown in 100 ml LB-Amp overnight at 37 °C with shaking at 600 rpm. The following day, I isolated the DNA of the correct plasmids again and purified it using the EndoFree® Plasmid Maxi Kit (Qiagen) to obtain endotoxin-free plasmid DNA ready for transfection.

Table 5. List of enzymes and buffers used for a control digest of the plasmids obtained by mini preparation.

Insert fragment	Restriction enzyme	Buffer
Nsp5	NdeI	Buffer O(10X) (Thermo Scientific)
Nsp13 aa 206-582	HindIII	Buffer R (10X) (Thermo Scientific)
C2	NdeI	Buffer O(10X) (Thermo Scientific)
C1r	SacI	Buffer SacI (10x) (Thermo Scientific)
C1s	PvuII	Buffer G (10x) (Thermo Scientific)
CFB	XhoI	Buffer R (10X) (Thermo Scientific)
CFD	XhoI	Buffer R (10X) (Thermo Scientific)
DDX3X	NdeI	Buffer O (10X) (Thermo Scientific)
DDX58	PvuII	Buffer G (10x) (Thermo Scientific)

3.2.2. Expression of recombinant antigens

I expressed recombinant NLuc-tagged (Promega) antigens in transiently transfected human HEK293 cells. I always performed the transfection as described in the following.

On Day 1, I seeded 600,000 cells per well onto a treated 6-well plate (Thermo Scientific). I cultured the cells in DMEM low glucose (Lonza) with 10% heat-inactivated FBS low IgG (Thermo Scientific), 1% L-Glutamine, and 1% Pen/Strep and incubated overnight at 37 °C.

On Day 2, after 24 hours, I transfected the cells using 2 µg of plasmid DNA. For the transfection reaction, I used 20 µl of Polyethylenimine (25KD, 10uM=250ug/ml) per 2 µg of DNA dissolved in 100 µl serum-free medium (Lonza). After the transfection reaction was incubated at RT for 10 min, I added it to the cells.

On Day 3, I checked the expression of the recombinant proteins via the detection of the EGFP signal. The GFP is encoded after the internal ribosomal binding site on the plasmid which allows for it to be transcribed independently from the tagged antigen.

On Day 4, 48 hours after the transfection, I harvested the proteins from the supernatant and upon cell lysis with 20% Triton X-100. I collected the culture supernatant and centrifuged it for 10 min at 300 g to remove cells from the supernatant. I filtered the supernatant through a 0,22 µm syringe filter (Sarstedt). Once the supernatant was collected, I added 400 µl of trypsin per well to detach the cells. The cells were incubated for 30 sec. I added 1 ml of culture medium to stop the reaction and collected the cells. I added 1.5 ml of culture media to the plate to collect any remaining cells and pooled it into

the tube with the collected cells. The cells were centrifuged at 300 g for 10 min at RT. I discarded the supernatant and resuspended the cell pellet in 1 ml PBS per tube. The resuspended cells were again centrifuged at 300 g for 10 min at RT. I again discarded the supernatant and resuspended the cell pellet in 100 μ l of lysis buffer (20 μ l of 1M Tris buffer, pH8, 35 μ l of 4M NaCl, 2 μ l of 500 mM EDTA, 50 μ l of Triton X-100, 10 μ l of phosphatase inhibitor, 10 μ l of protease inhibitor and water up to a final volume of 1 ml). The samples were incubated for 30 min on ice. Finally, the samples were centrifuged at 13,000 rpm for 30 min at 4 °C and I collected the supernatant containing the lysate proteins into a new precooled tube.

For the quantification of the expressed NLuc-protein in the supernatant and lysate, I measured the NLuc activity in 1 μ l-duplicates mixed with 25 μ l of TBST (20 mM Tris buffer, 150 mM NaCl, 0.5% Tween 20, pH 8) in white flat-bottom 96-well microplates (Perkin Elmer, Waltham, MA USA). Into each well 25 μ l of 1x TBST, I added 1 μ l of the supernatant sample or lysate sample, and 40 μ l of NanoGlo substrate (Promega) and incubated it for a few seconds protected from light on a rotary shaker at 600 rpm. I measured the activity with GloMax® Navigator (Promega) using the standard CellTiterGlo protocol (Promega). The proteins collected in lysate and supernatant were stored at -80 °C.

3.2.3. Luciferase Immunoprecipitation System (LIPS) assay

The luciferase immunoprecipitation system (LIPS) assay is an immunoassay used for the detection of antigen-specific (auto)antibodies. In principle, the antigen is fused to a luciferase reporter that emits luminescence which is measured to quantify the amount of antigen-specific antibodies in serum. In this thesis, the antigens were fused to a small nanoluciferase (NLuc) that emits bright bioluminescence. The NLuc-antigen fusion protein is incubated with sera from COVID-19 patients and sera from healthy donors as a control. During the incubation, the NLuc-antigen is recognized and bound by antigen-specific antibodies. Afterward, Sepharose A is added to capture the antibodies by binding the Fc region of the IgG antibodies. The sepharose beads bind all antibodies in the serum, i.e. both the free antibodies and the antibody-antigen complexes. The unbound antigen is removed by several washing steps. Finally, the relative amount of antibody bound to the NLuc-antigen is quantified by measuring the luminescence emitted by nanoluciferase after adding the NLuc substrate fumarazin (Figure 5) (Burbelo et al., 2009).

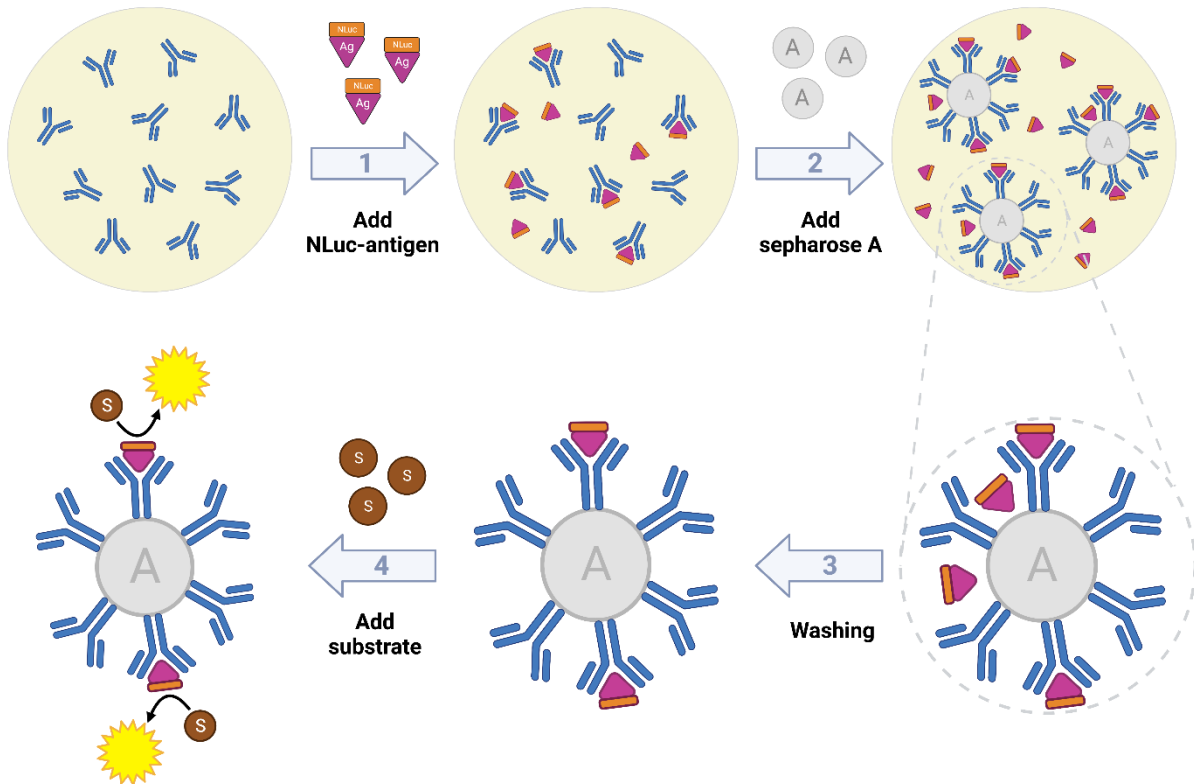


Figure 5. Overview of the LIPS assay. The antigen fused to nanoluciferase (NLuc) protein is added to the serum (1). During the incubation, the NLuc-antigen is recognized and bound by antigen-specific antibodies. After 2 hours at RT, sepharose A is added (2) to capture the antibodies by binding the Fc region of the IgG antibodies. The sepharose beads bind all antibodies in the serum, i.e. both the free antibodies and the antibody-antigen complexes. The unbound antigen is removed by several washing steps (3). Finally, the relative amount of antibody bound to the NLuc-antigen is quantified by measuring the luminescence emitted by nanoluciferase after adding the NLuc substrate fumarazin (4). Created in Biorender.

3.2.3.1. LIPS protocol

I added 25µl of the NLuc-tagged antigen in TBST containing 4mio LU (acceptance range 3.5×10^6 LU to 4.5×10^6 LU) to 1µl of the respective standard or serum sample into a 96-deep-well plate (Beckman-Coulter). After incubation for two hours at RT, I added 50 µl of rProtein A Sepharose™ Fast Flow slurry (Cat. GE17-1279-03, ThermoFisher Sci.) previously glycine-blocked and the reaction was incubated at 4 °C with shaking at 750 rpm. Afterward, I washed the unbound antigen five times with cold TBST, using the BioTeK ELx405 washer. In each washing step, I added 600 µl of TBST per well. I centrifuged the plates at 500 g for 3 min at 4 °C and aspirated the TBST to leave approx. 100 µl per well. Then, I manually transferred the Sepharose in approx. 100 µl TBST to a 96well Optiplate (PerkinElmer). I prepared the luciferase reagent by mixing 1 volume of Nano-Glo Luciferase Assay Substrate with 50 volumes of Nano-Glo Luciferase Assay Buffer (Cat. N112A & N113A, Promega) and 50 volumes of TBST. Finally, I added 40 µl of the luciferase reagent per well. I measured the light emission with the GloMax® Navigator (Promega) using the CellTiterGlo protocol (Promega). Each

sample was tested at least in duplicate. Measured light units (LU) were converted to AU using either a positive serum as an index or a serial dilution of antibody-positive serum.

3.2.4. Statistical analysis

The calibration curves and AU calculations were made using Excel 365 (Microsoft). The cutoff was set at 5 standard deviations (SD) above the mean of AU of the control group. The difference in antibody titers between groups was analyzed using a Kruskal–Wallis test, with $p < 0.05$, followed by Dunn’s multiple comparison test, with $\alpha < 0.05$. Antibody-positivity was analyzed between groups using Fisher’s exact test. All data statistics were performed using GraphPad Prism v.9.2.0 Software.

The antibody titers are shown as dots (individual values) and the median is shown as a line. Only significant comparisons between groups are shown.

4. Results

4.1. Production of nanoluciferase-tagged antigens

Recombinant plasmids pCMV6-SP-IL6-NLuc-antigen-IRES-GFP were made (Table 6, schematic of the cloned inserts is shown in Supplement 1), confirmed by Sanger sequencing, and transfected into human HEK293 cells. All NLuc-tagged antigens were successfully secreted into the culture supernatant and harvested from the cell lysate. All antigens had sufficient luciferase activity to continue with the LIPS assay (Table 7).

Table 6. List of cloned plasmids and concentrations of plasmid DNA obtained by maxi preparation using the EndoFree® Plasmid Maxi Kit (Qiagen). The plasmid DNA is endotoxin-free and ready for transfection.

Plasmid name	DNA concentration [ng/μl]
pCMV6_SP-IL6_NLuc_NSP5_IRES-GFP-Puro(END)	566
pCMV6_SP-IL6_NLuc_NSP13_206-582_IRES-GFP-Puro(END)	664
pCMV6_SP-IL6_NLuc_C2_IRES-GFP-Puro(END)	1098
pCMV6_SP-IL6_NLuc_C1r_IRES-GFP-Puro(END)	578
pCMV6_SP-IL6_NLuc_C1s_IRES-GFP-Puro(END)	551
pCMV6_SP-IL6_NLuc_CFB_IRES-GFP-Puro(END)	917
pCMV6_SP-IL6_NLuc_CFD_IRES-GFP-Puro(END)	373
pCMV6_SP-IL6_NLuc_DDX3X_IRES-GFP-Puro(END)	659
pCMV6_SP-IL6_NLuc_DDX58_IRES-GFP-Puro(END)	426

Table 7. NLuc activity of antigens harvested in cell lysate and culture supernatant.

SP-IL6-NLuc-Antigen	NLuc activity of the antigen [LU/μl]	
	Cell lysate	Supernatant
NSP5	688100000	2502000
NSP13 aa 206-582	421200000	6230000
C2	171350000	240150
C1r	35005000	1004150
C1s	62975000	299250
CFB	461600000	7855000
CFD	235900000	4305000
DDX3X	786550000	31440000
DDX58	329650000	917650

4.2. Establishment of standards for the LIPS assay

First, a standard to allow quantification of the antibodies was established. The antigens were tested in a LIPS assay using a serial dilution of a commercially available antigen-specific antibody and/or anti-NLuc antibody (Promega). All dilutions were made in healthy SARS-CoV-2 negative serum. The standard was tested with antigens harvested from the supernatant and the cell lysate. First, a dilution series of 1:100, 1:250, 1:500, 1:1,000, 1:2,000, 1:5,000, and 1:10,000 was tested. If necessary, higher and/or lower dilutions were tested until an optimal dilution range was reached. The \log_2 AU (y-axis) assigned to the antibody dilutions were plotted against the LU (x-axis) (Figure 6). An optimal dilution series and source of antigen (cell lysate or culture supernatant) were selected based on the R^2 values and curve fit of the constructed calibration curve. A summary of established standards for the precipitation of the newly produced SP-IL6-NLuc-antigens is given in Table 8.

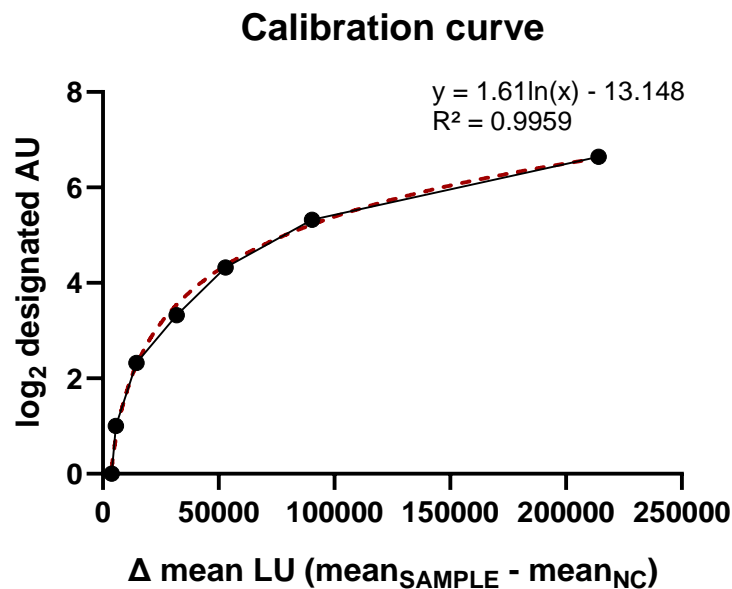


Figure 6. Representative example of a calibration curve used in the LIPS assay. \log_2 arbitrary units (AU) designated to the standard calibrators (y-axis) are plotted against the *delta mean LU* (x-axis). The red broken line represents a calibration curve obtained by nonlinear regression, $R^2=0.9959$. The equation of the calibration curve $y = 1.61\ln(x) - 13.148$ is used to convert LU (x) to AU (y).

Table 8. A summary of the established standards for the NLuc-tagged antigens used in the LIPS assay.

SP-IL6-NLuc-antigen	Source of antigen	Antibody used for the standard	Catalog number, company	Final dilution range of the antibody
NSP5	supernatant	anti-NLuc	N700A, Promega	1:50 - 1:10,000
NSP13 aa 206-582	supernatant	anti-NLuc	N700A, Promega	1:100 - 1:10,000
C2	cell lysate	anti-C2	RPA862Hu01, Cloud-Clone	1:2 - 1:500
C1r	supernatant	anti-NLuc	N700A, Promega	1:50 - 1:1,000
C1s	cell lysate	anti-C1s	MAB674Hu22, Cloud-Clone	1:2 - 1:5,000
CFB	cell lysate	anti-CFB	PAC011Hu01, Cloud-Clone	1:10 - 1:10,000
CFD	supernatant	anti-CFD	MAB833Hu22, Cloud-Clone	1:10 - 1:10,000
DDX3X	supernatant	anti-DDX3X	STJ112138-50, St John's Laboratory	1:2 - 1:100
DDX58	supernatant	anti-DDX58	MAB532Hu22, Cloud-Clone	1:5 - 1:10,000

The standard for measuring NP, RBD, and S2 antibodies as well as for IFN autoantibodies (IFN α 1, IFN α 8, IFN α 17, and IFN ω 1) was already established in the Bonifacio laboratory. Results for NP antibodies were converted to AU using a reference antibody positive index serum and a negative control serum (both provided by Helmholtz Zentrum in Munich) according to the formula: $(LU\ test\ serum - LU\ Negative\ Control\ serum) / (LU\ Positive\ index\ serum - LU\ Negative\ Control\ serum)$. For RBD and S2, positive serum diluted in SARS-CoV-2 negative healthy serum was used as standard (provided by Helmholtz Zentrum in Munich). For IFN α 1, IFN α 8, IFN α 17, and IFN ω 1 a serial dilution of antigen-specific antibodies in healthy human sera was used. AU for RBD and S2 antibodies and IFN autoantibodies was calculated using a calibration curve as already described for the newly established standards.

4.3. Detection of SARS-CoV-2 RBD, S2, and NP antibodies

As presumed, among the 100 healthy blood donors from May 2021, SARS-CoV-2 positive sera were detected: 11 (11%) NP+, 53 (53%) RBD+, 55 (55%) S2+ (Figure 7). Samples from 41 donors were negative for all three types of antibodies. These 41 donors were selected as a SARS-CoV-2 seronegative healthy control group that was used for the analysis of autoantibodies and NSP antibodies.

Expectedly, almost all sera from patients were positive for NP, RBD, and S2 antibodies: 38 (90.5%) NP+, 35 (83.3%) RBD+, 37 (88.1%) S2+ from the 42 moderate patients and 57 (98.3%) NP+, 58 (100%) RBD+, 57 (98.3%) S2+ from the 58 severe/critical patients. 35 (83.3%) of the moderate and 57 (98.3%) of the severe patients were positive for all three types of antibodies. Severe/critical patients had significantly higher RBD and S2 antibody titers compared to the moderate ones (RBD $p < 0.0001$, S2 $p = 0.0038$), whereas no significant difference was observed for the NP antibody titers ($p = 0.1607$).

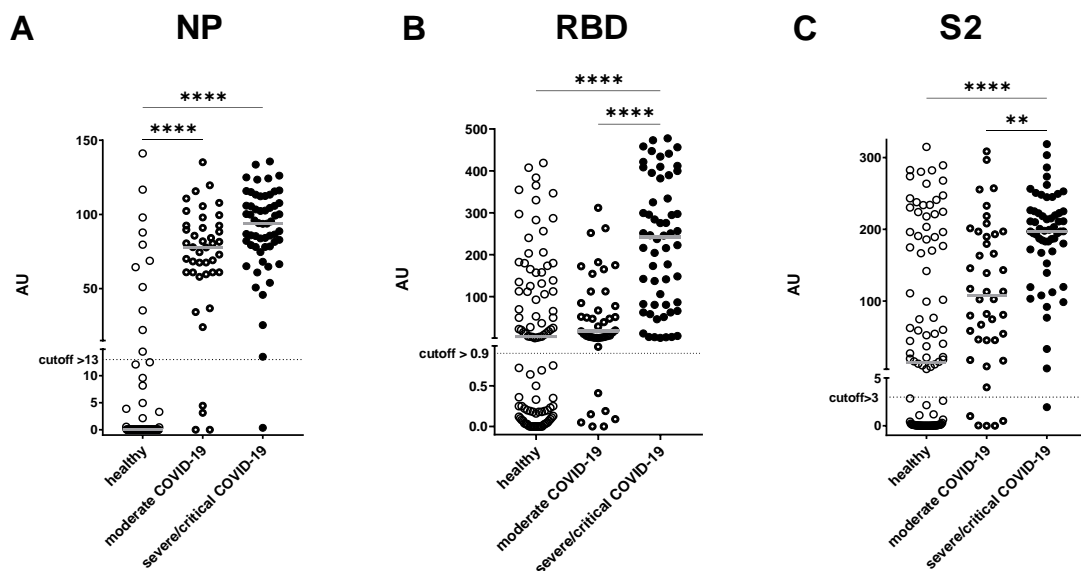


Figure 7. SARS-COV-2 NP (A), RBD (B), and S2 (C) antibody titers in 42 moderate COVID-19 patients, 58 severe/critical COVID-19 patients, and 100 healthy blood donors sampled in May 2021. The broken lines show cutoffs at 13 AU, 0.9 AU, and 3 AU for NP, RBD, and S2, respectively. The thin-lined open circles represent the group of healthy blood donors, the thick-lined open circles the patients with moderate COVID-19, and the full circles the patients with severe/critical COVID-19. Each point is an individual and the horizontal bar indicates the median. The antibody titers were compared between groups by the Kruskal-Wallis test followed by Dunn's multiple comparison test, with $\alpha < 0.05$. Only statistically significant comparisons are shown.

4.4. Autoantibodies specific for inflammation-associated proteins

Autoantibodies are hypothesized to play a role in the pathogenesis of COVID-19 and are associated with disease severity. The main objective was to detect various autoantibodies specific for inflammation-associated proteins in sera from SARS-CoV-2 positive patients and investigate a potential association of the autoantibodies with the disease severity by comparing the number of autoantibody-positive individuals between groups of moderate and severe/critical COVID-19 patients. Samples of 41 SARS-CoV-2 seronegative healthy blood donors were tested as controls for the analysis of autoantibodies. The cutoff was set at 5 standard deviations (SD) above the mean of AU of the control group. At least one type of autoantibody was detected in 51% of the COVID-19 patients and 12.2% of the controls (Figure 8).

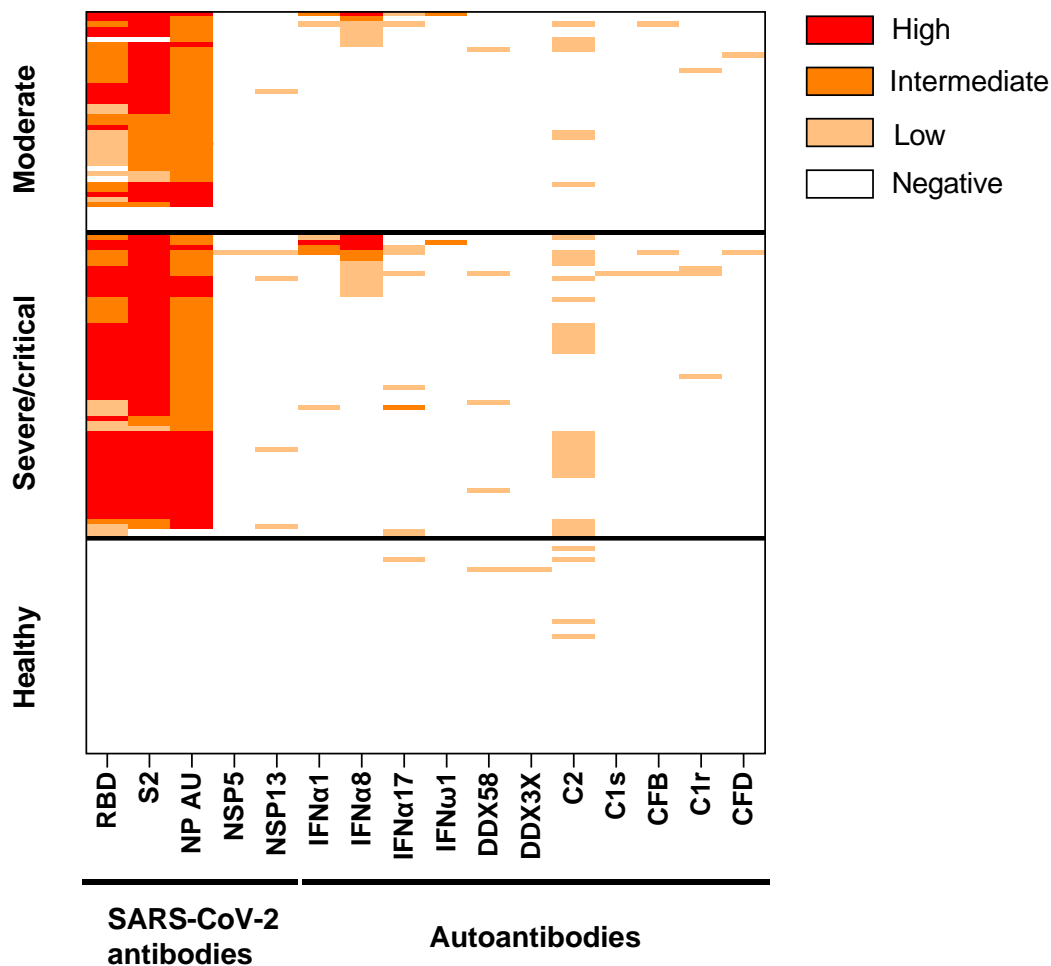


Figure 8. Heatmap of SARS-CoV-2 antibodies and autoantibodies among 42 moderate COVID-19 patients, 58 severe/critical COVID-19 patients, and 41 healthy SARS-CoV-2 seronegative blood donors sampled in May 2021. The (auto)antibody-positive samples were arbitrarily categorized as low (≤ 10 AU), intermediate (between 10 and 100 AU), and high (≥ 100 AU). Each column represents a certain (auto)antibody and one row represents one patient.

4.4.1. IFN autoantibodies

The sera were tested in a panel of LIPS assays for four types of IFN autoantibodies (IFN α 1, IFN α 8, IFN α 17, and IFN ω 1). None of the IFN α 1, IFN α 8, and IFN ω 1 autoantibodies were detected in the control group, while one control serum was positive for IFN α 17 with a very low autoantibody titer of 0.24 AU (Figure 9). In contrast, all four types of autoantibodies were detected in sera from patients. Overall, 22% of COVID-19 patients were positive for at least one type of IFN autoantibody. In contrast, only 2.4% of the healthy controls had IFN autoantibodies, hence, there is a higher prevalence of IFN autoantibodies in hospitalized COVID-19 patients compared to the healthy SRAS-CoV-2 seronegative individuals. However, no significant difference was found between groups of moderate and severe/critical patients (Table 9). At least one type of IFN autoantibody was detected in 16.7% of moderate patients and 25.9% of severe/critical patients ($p=0.3329$). Almost a third of the 22 IFN autoantibody-positive samples were positive for more than one type of IFN autoantibody: seven of the 22 positive patients were positive for IFN α 1 and IFN α 8 antibodies, and four of the seven anti-IFN α 1+ anti-IFN α 8+ were also positive for IFN α 17 autoantibodies. Only one patient had all four types of IFN autoantibodies. Surprisingly, this patient had moderate COVID-19. The IFN ω 1 autoantibodies were detected only in two patients, the one that was positive for all four autoantibodies and one severe patient. IFN autoantibodies were found in 9 female and 13 male patients, aged from 44 to 82 years. There was no relationship between the sex or age of the patients.

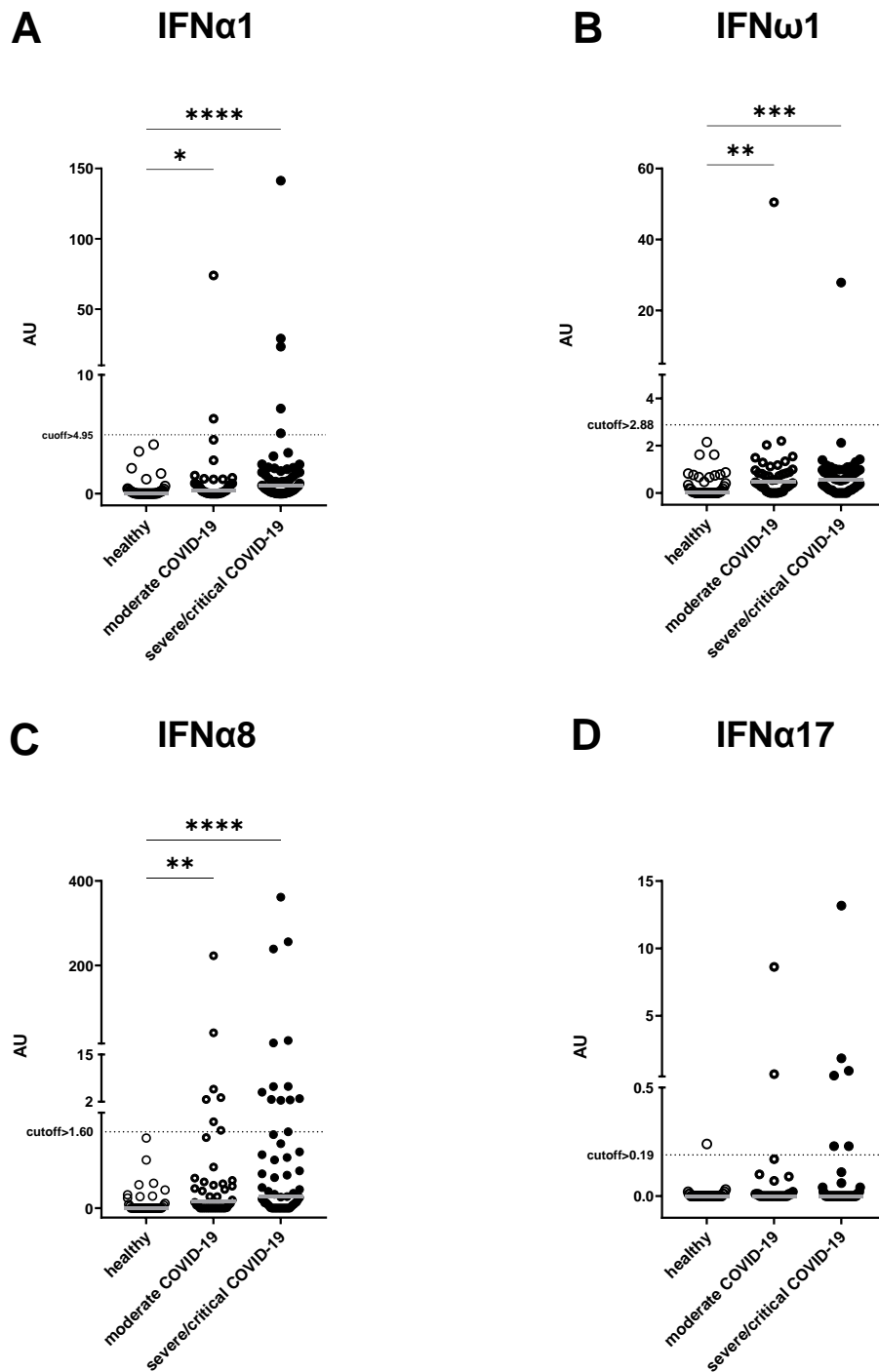


Figure 9. Titers of IFN autoantibodies specific for IFN α 1 (A), IFN ω 1 (B), IFN α 8 (C), and IFN α 17 (D) in 42 moderate COVID-19 patients, 58 severe/critical COVID-19 patients and 41 SARS-CoV-2 seronegative healthy blood donors sampled in May 2021. The broken lines show cutoffs for antigens IFN α 1, IFN ω 1, IFN α 8, and IFN α 17 at 4.95 AU, 2.88 AU, 1.60 AU, and 0.19 AU, respectively. The thin-lined open circles represent the group of healthy blood donors, the thick-lined open circles represent the patients with moderate COVID-19 and the full circles represent the patients with severe/critical COVID-19. Each point is an individual and the horizontal bar indicates the median. The antibody titers were compared between groups by the Kruskal-Wallis test followed by Dunn’s multiple comparison test, with $\alpha < 0.05$. Only statistically significant comparisons are shown.

Table 9. Distribution of IFN autoantibodies in COVID-19 patients. P-values were calculated using Fisher’s exact test with a two-tailed p-value <0.05.

Factor	Category	IFN autoantibody-positive*	p-value
Disease severity	Moderate (N=42)	7 (16.7%)	0.3329
	Severe/critical (N=58)	15 (25.9%)	
Sex	Female (N=41)	9 (22.0%)	>0.9999
	Male (N=59)	13 (22.0%)	
Age	≥65 (N=50)	10 (20.0%)	0.8097
	<65 (N=50)	12 (24%)	

*Positive for at least one of the four tested IFN autoantibodies.

4.4.2. Complement and DDX autoantibodies

The sera were also tested in a panel of LIPS assays for autoantibodies specific for complement proteins C2, C1r, C1s, CFB, CFD, and DDX helicases DDX3X and DDX58 (Figure 10). The DDX58, C1s, and C1r autoantibodies were detected in a few positive samples with antibody titers up to a maximum of 0.92 AU, 0.15 AU, and 0.34 AU, respectively. All patients were negative for DDX3X autoantibodies. The CFB and CFD autoantibodies were also rare and in very low titers, however, one outlier for each was detected with an antibody titer of 8.80 AU and 3.35 AU, respectively. Nonetheless, these samples were also considered low positive (<10 AU). The C2 autoantibodies were detected in 31% of the COVID-19 patients in contrast to the 9.8% of the controls. Moreover, the severe patients had significantly higher C2 autoantibody titers compared to the moderate ones (p=0.0002). However, like for the rest of the complement and DDX helicase autoantibodies, the C2 antibody titers were low, with a maximum antibody titer of 2.58 AU detected. In summary, the complement and DDX helicase-specific autoantibodies were rare and/or had very low titers (<10 AU). Therefore, they were not further analyzed.

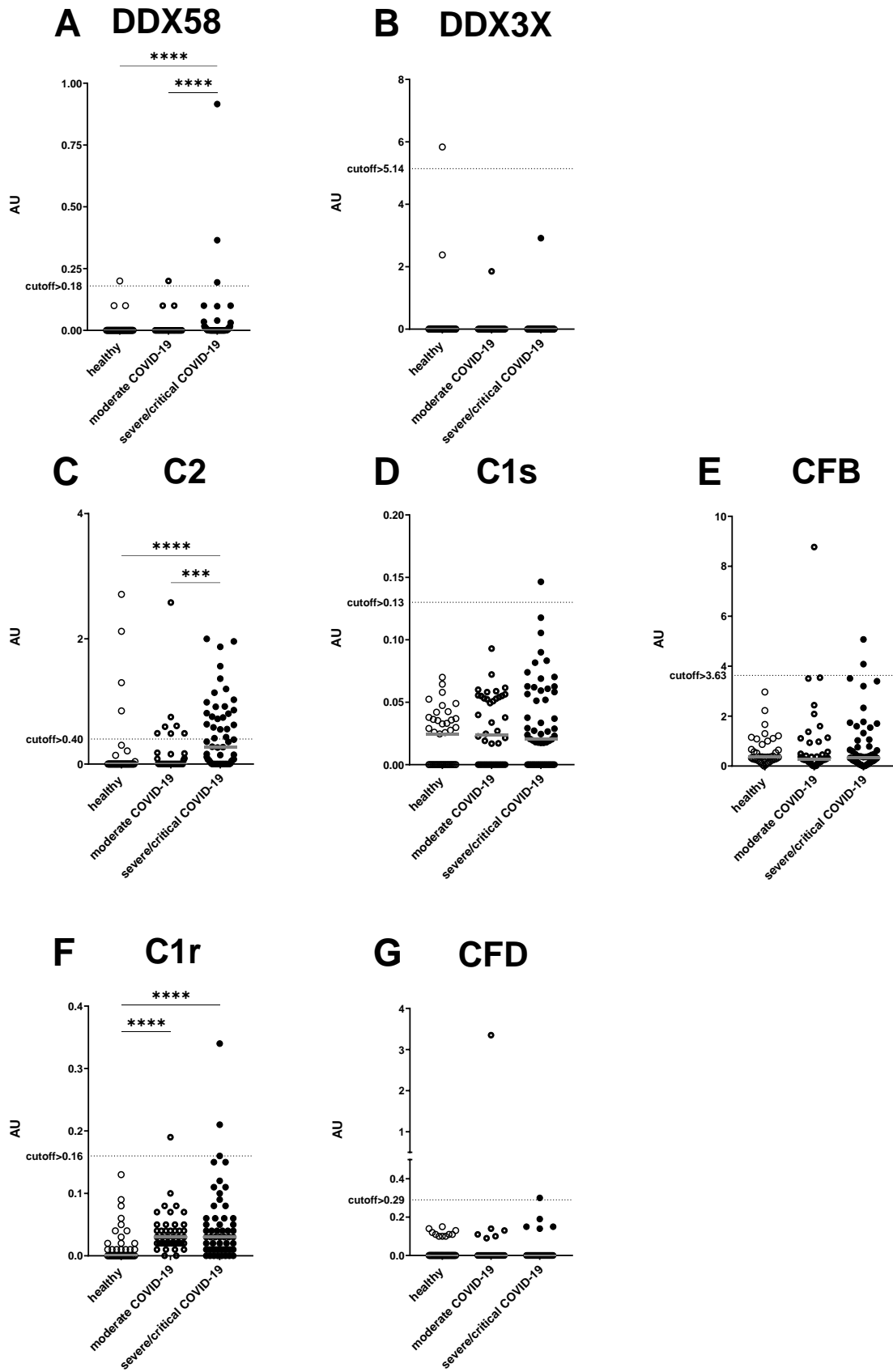


Figure 10. (Description on next page)

Figure 10. Titers of complement and DDX helicase autoantibodies specific for DDX58 (A), DDX3X (B), C2 (C), C1s (D), CFB (E), C1r (F), and CFD (G) in 42 moderate COVID-19 patients, 58 severe/critical COVID-19 patients, and 41 SARS-CoV-2 seronegative healthy blood donors. The broken lines show cutoffs for antigens DDX58, DDX3X, C2, C1s, CFB, C1r, and CFD at 0.18 AU, 5.14 AU, 0.40 AU, 0.13 AU, 3.63 AU, 0.16 AU, and 0.29 AU, respectively. The thin-lined open circles represent the group of healthy blood donors, the thick-lined open circles represent the patients with moderate COVID-19 and the full circles represent the patients with severe/critical COVID-19. Each point is an individual and the horizontal bar indicates the median. The antibody titers were compared between groups by the Kruskal-Wallis test followed by Dunn's multiple comparison test, with $\alpha < 0.05$. Only statistically significant comparisons are shown.

4.5. Detection of SARS-CoV-2 NSP antibodies

To assess structural mimicry between complement proteins or DDX helicases and SARS-CoV-2 proteins, in this study the NSP5 and NSP13 antigens were tested. All of the 41 healthy SARS-CoV-2 seronegative blood donors were negative for NSP antibodies implying a 100% specificity of the assay with the calculated cutoff values (Figure 11). However, almost all of the patients' sera were negative as well, except for one positive anti-NSP5 and four positive anti-NSP13 samples (Figure 8). Overall, the titer of the detected NSP5 and NSP13 antibodies was very low ranging from 0 AU to 1.82 AU and 0 AU to 3.51 AU for NSP5 and NSP13, respectively. Noteworthy, the five anti-NSP13 positive samples were also positive for the other SARS-CoV-2 antibodies but none of the DDX helicase autoantibodies (Figure 8). The one anti-NSP5 positive sample had low anti-C2 autoantibody titers but none of the remaining complement antibody-positive samples were positive for anti-NSP5. Since only one sample had antibodies against both proteins of the mimicked pair, no correlation analysis of the mimicked pair-specific antibodies could be done. Overall, the NSP antibodies were scarce in sera from COVID-19 patients and at very low titers.

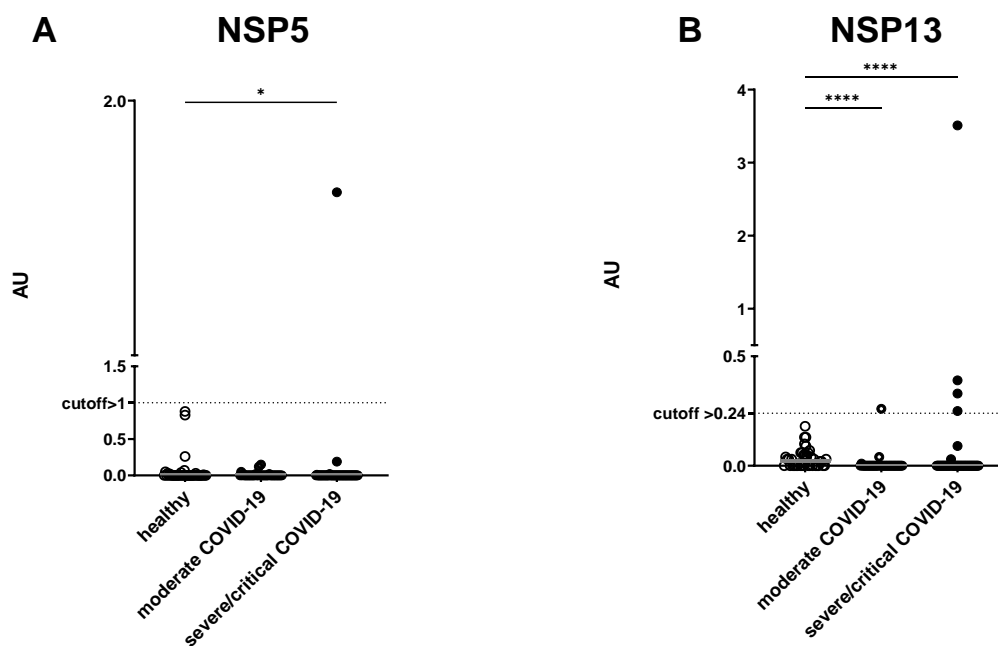


Figure 11. SARS-CoV-2 NSP5 (A) and NSP13 (B) antibody titers in 42 moderate COVID-19 patients, 58 severe/critical COVID-19 patients, and 41 healthy SARS-CoV-2 seronegative blood donors sampled in May 2021. The broken lines show cutoffs at 1.00 AU and 0.24 AU for NSP5 and NSP13 respectively. The thin-lined open circles represent the group of healthy blood donors, the thick-lined open circles the patients with moderate COVID-19, and the full circles the patients with severe/critical COVID-19. Each point is an individual and the horizontal bar indicates the median. The antibody titers were compared between groups by the Kruskal-Wallis test followed by Dunn's multiple comparison test, with $\alpha < 0.05$. Only statistically significant comparisons are shown.

5. Discussion

This thesis aimed to investigate the prevalence of autoantibodies specific for various inflammation-associated proteins in COVID-19 patients. Indeed, complement, DDX helicase and IFN autoantibodies were detected in the majority of the patients (51%). The rest of the patients (49%) were negative for all of the tested autoantibodies. A higher prevalence of autoantibodies was observed in COVID-19 patients in contrast to the SARS-CoV-2 seronegative controls (12.2%). However, only 8% of the patients had high or intermediate IFN autoantibody titers, whereas, the rest of the autoantibody-positive samples (43%) had very low autoantibody titers. Furthermore, as autoantibodies have been widely hypothesized of posing a risk for a more severe disease outcome, the association between IFN autoantibodies and disease severity was investigated. In addition, as IFN autoantibodies were reported to be more frequent in older men (Bastard et al., 2020), the effect of sex and age was also considered. Results showed no association of IFN autoantibodies with age, sex, or disease severity contrary to the previous reports. Furthermore, the sera were tested for SARS-CoV-2 NSP5 and NPS13 antibodies because their specific targets were mapped as mimicked pairs of the tested complement and DDX helicase antigens (Lasso et al., 2021). Similarly to most of the tested complement and DDX helicase autoantibodies, the NSP5 and NSP13 antibodies were rare (in only 5% of the patients) and in very low titers.

First, all samples were tested for SARS-CoV-2 RBD, S2, and NP antibodies. A SARS-CoV-2 seronegative control group was formed from 41 donors negative for all three of the tested antibodies. Expectedly, almost all of the COVID-19 patients were positive for the SARS-CoV-2 NP and S antibodies, with an exception of a few negative patients. These patients were likely sampled early post-symptom onset, therefore, it might have been too early to detect the SARS-CoV-2 antibodies. In accordance with previous reports (Hansen et al., 2021), higher titers were detected in severe/critical patients compared to moderate ones, especially for S protein.

Previous studies have reported an association between IFN autoantibodies and disease severity. In these studies, IFN autoantibodies were specific for groups of patients with severe and life-threatening COVID-19 in contrast to the asymptomatic, mild, and moderate patients (Bastard et al., 2020, Wang et al., 2021). The results of this thesis are somewhat in accordance with their findings as a higher prevalence of IFN autoantibodies was found in patients in comparison to the “unexposed” healthy donors, but no difference was observed between the moderate and severe/critical patients. Nonetheless, it needs to be emphasized that in the previous studies patients with moderate COVID-19 were either not included (Bastard et al., 2020) or were categorized by different criteria from the ones in this thesis (Wang et al., 2021). The moderate patients in this thesis have symptoms of mild pneumonia and may have received antibiotics, corticosteroids, or antiviral drugs approved for the treatment of COVID-19 such as remdesivir and paxlovid (Clinical Spectrum - COVID-19 Treatment Guidelines, 2022), but no

oxygen therapy. Importantly, these patients are at high risk of progressing to severe COVID-19. Overall, this thesis shows that the IFN autoantibodies are present not only in life-threatening but also in moderate “potentially severe” patients without any significant difference in prevalence between the two groups. Thus, the results are suggestive of IFN autoantibodies being a potential biomarker of not only the severe and life-threatening COVID-19, as already reported, but also for moderate patients, i.e. “potentially severe” ones. Worth mentioning that there is a need for a uniform categorization of COVID-19 for better comparison of the reported findings between studies.

In contrast, less is known about the other measured autoantibodies in COVID-19 patients. In their high-throughput autoantibody screening, among others (cytokines, chemokines, and cell-surface proteins), Wang et al. also found complement autoantibodies (C1qB, C6, and C7) (Wang et al., 2021). Notably, none were detected in the severe patients, and only a few were detected in the moderate patients. Similarly, this thesis also showed a low prevalence of the complement (except anti-C2) and DDX helicase autoantibodies in COVID-19; moreover, the measured titers of these autoantibodies were very low. Interestingly, a high prevalence of low-titer C2 autoantibodies was observed in COVID-19 patients, particularly in the severe/critical ones. Considering that autoantibodies can take a long time to develop, the C2 autoantibodies are interesting as there is a possibility that these low-titer autoantibodies could be newly induced by the viral infection. To clarify this presumption, testing follow-up samples is necessary. However, since only low-titer complement and DDX helicase autoantibodies were detected, there is a risk that false positives were detected. Therefore, the sensitivity of the assay should be tested by measuring the autoantibodies in previously described sera. On the other hand, the positive samples could be tested by other immunoassays to confirm the presence of the detected autoantibody. In contrast to the IFN autoantibodies, these autoantibodies cannot be considered as predictive or diagnostic markers of COVID-19.

In general, unlike the abundant reports of NP and S antibodies in COVID-19 patients, reports of NSP5 and NSP13 antibodies are scarce. In theory, the non-structural proteins should only be exposed to the immune system in infected cells and not virions. Thus, the non-structural proteins are expected to be less potent in triggering an antibody response in contrast to the more abundant and immunogenic structural proteins. In a comprehensive study of the IgG and IgM epitope landscape of the SARS-CoV-2 proteins epitope profiles of NSP proteins were described. Interestingly, they found the NSPs to have more IgM- epitopes than tIgG epitopes, in contrast to the NP and Spike proteins, which have more IgG- epitopes than IgM epitopes. It should be noted that the majority of the IgG epitopes of NSP13 are present in the zinc-binding domain (aa 1-100) (Cheng et al., 2021). The NSP13 (aa 206-582) antigen used in this study is missing the zinc-binding domain, and thus may not be the best antigen for the detection of NSP13 IgG antibodies. A study reported that 10.5% of COVID-19 patients had NSP5 antibodies (Hacim et al., 2021) which is approximately 10 times more than what was detected in our case. Considering that only the anti-NLuc antibody was used for the establishment of standards in LIPS

assays for NSP antibodies and the antigen-specific antibody was not tested, there is a possibility that the antigen is not folding correctly and cannot be recognized by the specific antibodies. However, based on previous evidence it is more likely that these proteins have very low antigenicity, thus, antibodies specific for them are rare. To exclude any cross-reactivity between the mimicked proteins, testing for autoreactive T cells should also be considered.

This study has several limitations. The number of subjects is relatively small and no longitudinal samples were tested. Ideally, samples of more diverse disease severity would be tested including a large set of asymptomatic, mild, moderate, severe, and critical cases to better clarify the severity of the risk these autoantibodies pose in COVID-19. Since it is still unclear whether these autoantibodies pre-exist or are induced by the SARS-CoV-2 infection, testing of follow-up samples is necessary. Without knowing whether the titer of these antibodies rises with time post-infection, it is difficult to determine whether the low-titer autoantibody-positive samples are truly positive. This is especially important in the testing of the post-infection-induced autoantibodies hypothesized to arise due to molecular mimicry. Furthermore, the effect of other viral infections should also be considered as studies have reported a comparable prevalence of autoantibodies not only in COVID-19 but also in other infectious diseases (Feng et al., 2022). Apart from sex and age, more metadata should be considered for the analysis. It is important to check for comorbidities such as autoimmune or malignant conditions, as well as to determine the therapies other than oxygenation the patients received when they were hospitalized. Also, the time interval between symptom onset and sampling should be considered. Subsequently, the positive patients should be tested for neutralizing autoantibodies to better understand the role of these autoantibodies in the pathogenesis of COVID-19. Lastly, the panel of antigens used in LIPS assay should be expanded by including other known targets of autoimmunity which would give a broader image of the general prevalence of autoantibodies in COVID-19 patients.

6. Conclusion

In conclusion, results are suggestive of IFN autoantibodies being a potential prognostic marker of not only the severe and life-threatening COVID-19 as already reported but also for moderate patients, i.e. the “potentially severe” ones. Overall, low titers of complement and DDX helicase autoantibodies were detected, hence, the presence of these autoantibodies cannot be considered a relevant prognostic or diagnostic marker of the disease. Similarly, the NSP proteins seem to have low antigenicity, and antibodies specific for them are scarce in comparison to the highly prevalent S and NP antibodies in serum from COVID-19 patients. Nonetheless, the findings imply autoantibodies to be more prevalent in serum from hospitalized COVID-19 patients making a rational presumption of autoantibodies to be an important factor in COVID-19. Altogether, results implicate autoantibodies should be further investigated for their role in the pathogenesis of COVID-19.

7. References

- Abdelrahman, Z., Li, M., & Wang, X. (2020). Comparative Review of SARS-CoV-2, SARS-CoV, MERS-CoV, and Influenza A Respiratory Viruses. *Frontiers in immunology*, *11*, 552909. <https://doi.org/10.3389/fimmu.2020.552909>
- Aoki, S. (1999). Rheumatoid arthritis and enteric bacteria. *Japanese Journal of Rheumatology* *9*, 325–352. <https://doi.org/10.1007/BF03041347>
- Bastard, P., Rosen, L. B., Zhang, Q., Michailidis, E., Hoffmann, H. H., Zhang, Y., Dorgham, K., Philippot, Q., Rosain, J., Béziat, V., Manry, J., Shaw, E., Haljasmägi, L., Peterson, P., Lorenzo, L., Bizien, L., Trouillet-Assant, S., Dobbs, K., de Jesus, A. A., Belot, A., ... Casanova, J. L. (2020). Autoantibodies against type I IFNs in patients with life-threatening COVID-19. *Science (New York, N.Y.)*, *370*(6515), eabd4585. <https://doi.org/10.1126/science.abd4585>
- Bates, T. A., Weinstein, J. B., Farley, S. E., Leier, H. C., Messer, W. B., & Tafesse, F. G. (2020). Cross-reactivity of SARS-CoV structural protein antibodies against SARS-CoV-2. *bioRxiv: the preprint server for biology*, 2020.07.30.229377. <https://doi.org/10.1101/2020.07.30.229377>
- Baum, H., Brusica, V., Choudhuri, K., Cunningham, P., Vergani, D., & Peakman, M. (1995). MHC molecular mimicry in diabetes. *Nature medicine*, *1*(5), 388. <https://doi.org/10.1038/nm0595-388>
- Boechat, J. L., Chora, I., Morais, A., & Delgado, L. (2021). The immune response to SARS-CoV-2 and COVID-19 immunopathology - Current perspectives. *Pulmonology*, *27*(5), 423–437. <https://doi.org/10.1016/j.pulmoe.2021.03.008>
- Burbelo, P. D., Ching, K. H., Klimavicz, C. M., & Iadarola, M. J. (2009). Antibody profiling by Luciferase Immunoprecipitation Systems (LIPS). *Journal of visualized experiments: JoVE*, (32), 1549. <https://doi.org/10.3791/1549>
- Calkovska, A., Kolomaznik, M., & Calkovsky, V. (2021). Alveolar type II cells and pulmonary surfactant in COVID-19 era. *Physiological research*, *70*(S2), S195–S208. <https://doi.org/10.33549/physiolres.934763>
- Cervia, C., Zurbuchen, Y., Taeschler, P., Ballouz, T., Menges, D., Hasler, S., Adamo, S., Raeber, M. E., Bächli, E., Rudiger, A., Stüssi-Helbling, M., Huber, L. C., Nilsson, J., Held, U., Puhan, M. A., & Boyman, O. (2022). Immunoglobulin signature predicts risk of post-acute COVID-19 syndrome. *Nature communications*, *13*(1), 446. <https://doi.org/10.1038/s41467-021-27797-1>

- Cheng, L., Zhang, X., Chen, Y., Wang, D., Zhang, D., Yan, S., Wang, H., Xiao, M., Liang, T., Li, H., Xu, M., Hou, X., Dai, J., Wu, X., Li, M., Lu, M., Wu, D., Tian, R., Zhao, J., Zhang, Y., ... Zhang, S. (2021). Dynamic landscape mapping of humoral immunity to SARS-CoV-2 identifies non-structural protein antibodies associated with the survival of critical COVID-19 patients. *Signal transduction and targeted therapy*, 6(1), 304. <https://doi.org/10.1038/s41392-021-00718-w>
- Feng, A., Yang, E., Moore, A., Dhingra, S., Chang, S., Yin, X., Pi, R., Mack, E., Völkel, S., Geßner, R., Gundisch, M., Neubauer, A., Renz, H., Tsiodras, S., Fragkou, P., Asuni, A., Levitt, J., Wilson, J., Leong, M., Lumb, J., ... Utz, P. (2022). Autoantibodies targeting cytokines and connective tissue disease autoantigens are common in acute non-SARS-CoV-2 infections. Research square, rs.3.rs-1233038. <https://doi.org/10.21203/rs.3.rs-1233038/v1>
- Grobben, M., van der Straten, K., Brouwer, P. J., Brinkkemper, M., Maisonnasse, P., Dereuddre-Bosquet, N., Appelman, B., Lavell, A. A., van Vught, L. A., Burger, J. A., Poniman, M., Oomen, M., Eggink, D., Bijl, T. P., van Willigen, H. D., Wynberg, E., Verkaik, B. J., Figaroa, O. J., de Vries, P. J., Boertien, T. M., ... van Gils, M. J. (2021). Cross-reactive antibodies after SARS-CoV-2 infection and vaccination. *eLife*, 10, e70330. <https://doi.org/10.7554/eLife.70330>
- Hadjadj, J., Yatim, N., Barnabei, L., Corneau, A., Boussier, J., Smith, N., Péré, H., Charbit, B., Bondet, V., Chenevier-Gobeaux, C., Breillat, P., Carlier, N., Gauzit, R., Morbieu, C., Pène, F., Marin, N., Roche, N., Szwebel, T. A., Merklings, S. H., Treluyer, J. M., ... Terrier, B. (2020). Impaired type I interferon activity and inflammatory responses in severe COVID-19 patients. *Science (New York, N.Y.)*, 369(6504), 718–724. <https://doi.org/10.1126/science.abc6027>
- Hansen, C. B., Jarlhelt, I., Pérez-Alós, L., Hummelshøj Landsy, L., Loftager, M., Rosbjerg, A., Helgstrand, C., Bjelke, J. R., Egebjerg, T., Jardine, J. G., Sværke Jørgensen, C., Iversen, K., Bayarri-Olmos, R., Garred, P., & Skjoedt, M. O. (2021). SARS-CoV-2 Antibody Responses Are Correlated to Disease Severity in COVID-19 Convalescent Individuals. *Journal of immunology (Baltimore, Md. : 1950)*, 206(1), 109–117. <https://doi.org/10.4049/jimmunol.2000898>
- Hippich, M., Sifft, P., Zapardiel-Gonzalo, J., Böhmer, M. M., Lampasona, V., Bonifacio, E., & Ziegler, A. G. (2021). A public health antibody screening indicates a marked increase of SARS-CoV-2 exposure rate in children during the second wave. *Med (New York, N.Y.)*, 2(5), 571–572. <https://doi.org/10.1016/j.medj.2021.03.019>
- Hu, B., Huang, S., & Yin, L. (2021). The cytokine storm and COVID-19. *Journal of medical virology*, 93(1), 250–256. <https://doi.org/10.1002/jmv.26232>
- Huang, Y., Yang, C., Xu, X. F., Xu, W., & Liu, S. W. (2020). Structural and functional properties of SARS-CoV-2 spike protein: potential antiviral drug development for COVID-19. *Acta pharmacologica Sinica*, 41(9), 1141–1149. <https://doi.org/10.1038/s41401-020-0485-4>

- Jiang, H. W., Li, Y., Zhang, H. N., Wang, W., Yang, X., Qi, H., Li, H., Men, D., Zhou, J., & Tao, S. C. (2020). SARS-CoV-2 proteome microarray for global profiling of COVID-19 specific IgG and IgM responses. *Nature communications*, *11*(1), 3581. <https://doi.org/10.1038/s41467-020-17488-8>
- Kaeuffer, C., Le Hyaric, C., Fabacher, T., Mootien, J., Dervieux, B., Ruch, Y., Hugerot, A., Zhu, Y. J., Pointurier, V., Clere-Jehl, R., Greigert, V., Kassegne, L., Lefebvre, N., Gallais, F., Covid Alsace Study Group, Meyer, N., Hansmann, Y., Hirschberger, O., Danion, F., & COVID Alsace Study Group (2020). Clinical characteristics and risk factors associated with severe COVID-19: prospective analysis of 1,045 hospitalised cases in North-Eastern France, March 2020. *Euro surveillance : bulletin Europeen sur les maladies transmissibles = European communicable disease bulletin*, *25*(48), 2000895. <https://doi.org/10.2807/1560-7917.ES.2020.25.48.2000895>
- Khamsi R. (2021). Rogue antibodies could be driving severe COVID-19. *Nature*, *590*(7844), 29–31. <https://doi.org/10.1038/d41586-021-00149-1>
- Kuo, Y. B., Chang, C. A., Wu, Y. K., Hsieh, M. J., Tsai, C. H., Chen, K. T., Chen, C. Y., & Chan, E. C. (2010). Identification and clinical association of anti-cytokeratin 18 autoantibody in COPD. *Immunology letters*, *128*(2), 131–136. <https://doi.org/10.1016/j.imlet.2009.12.017>
- Lasso, G., Honig, B., & Shapira, S. D. (2021). A Sweep of Earth's Virome Reveals Host-Guided Viral Protein Structural Mimicry and Points to Determinants of Human Disease. *Cell systems*, *12*(1), 82–91.e3. <https://doi.org/10.1016/j.cels.2020.09.006>
- Lebar, R., Baudrimont, M., & Vincent, C. (1989). Chronic experimental autoimmune encephalomyelitis in the guinea pig. Presence of anti-M2 antibodies in central nervous system tissue and the possible role of M2 autoantigen in the induction of the disease. *Journal of autoimmunity*, *2*(2), 115–132. [https://doi.org/10.1016/0896-8411\(89\)90149-2](https://doi.org/10.1016/0896-8411(89)90149-2)
- Li F. (2016). Structure, Function, and Evolution of Coronavirus Spike Proteins. *Annual review of virology*, *3*(1), 237–261. <https://doi.org/10.1146/annurev-virology-110615-042301>
- Li, M. Y., Li, L., Zhang, Y., & Wang, X. S. (2020). Expression of the SARS-CoV-2 cell receptor gene ACE2 in a wide variety of human tissues. *Infectious diseases of poverty*, *9*(1), 45. <https://doi.org/10.1186/s40249-020-00662-x>
- Liu, W., Liu, L., Kou, G., Zheng, Y., Ding, Y., Ni, W., Wang, Q., Tan, L., Wu, W., Tang, S., Xiong, Z., & Zheng, S. (2020). Evaluation of Nucleocapsid and Spike Protein-Based Enzyme-Linked Immunosorbent Assays for Detecting Antibodies against SARS-CoV-2. *Journal of clinical microbiology*, *58*(6), e00461-20. <https://doi.org/10.1128/JCM.00461-20>
- Liu, Y., Sawalha, A. H., & Lu, Q. (2021). COVID-19 and autoimmune diseases. *Current opinion in rheumatology*, *33*(2), 155–162. <https://doi.org/10.1097/BOR.0000000000000776>

- Malone, B., Urakova, N., Snijder, E. J., & Campbell, E. A. (2022). Structures and functions of coronavirus replication-transcription complexes and their relevance for SARS-CoV-2 drug design. *Nature reviews. Molecular cell biology*, 23(1), 21–39. <https://doi.org/10.1038/s41580-021-00432-z>
- Maoz-Segal, R., & Andrade, P. (2015). Molecular Mimicry and Autoimmunity. *Infection and Autoimmunity*, 27–44. <https://doi.org/10.1016/B978-0-444-63269-2.00054-4>
- Martínez-Flores, D., Zepeda-Cervantes, J., Cruz-Reséndiz, A., Aguirre-Sampieri, S., Sampieri, A., & Vaca, L. (2021). SARS-CoV-2 Vaccines Based on the Spike Glycoprotein and Implications of New Viral Variants. *Frontiers in immunology*, 12, 701501. <https://doi.org/10.3389/fimmu.2021.701501>
- Matyushkina, D., Shokina, V., Tikhonova, P., Manuvera, V., Shirokov, D., Kharlampieva, D., Lazarev, V., Varizhuk, A., Vedekhina, T., Pavlenko, A., Penkin, L., Arapidi, G., Pavlov, K., Pushkar, D., Kolontarev, K., Rummyantsev, A., Rummyantsev, S., Rychkova, L., & Govorun, V. (2022). Autoimmune Effect of Antibodies against the SARS-CoV-2 Nucleoprotein. *Viruses*, 14(6), 1141. <https://doi.org/10.3390/v14061141>
- McClain, M. T., Heinlen, L. D., Dennis, G. J., Roebuck, J., Harley, J. B., & James, J. A. (2005). Early events in lupus humoral autoimmunity suggest initiation through molecular mimicry. *Nature medicine*, 11(1), 85–89. <https://doi.org/10.1038/nm1167>
- McGill, J. R., Lagassé, H., Hernandez, N., Hopkins, L., Jankowski, W., McCormick, Q., Simhadri, V., Golding, B., & Sauna, Z. E. (2022). A structural homology approach to identify potential cross-reactive antibody responses following SARS-CoV-2 infection. *Scientific reports*, 12(1), 11388. <https://doi.org/10.1038/s41598-022-15225-3>
- McNab, F., Mayer-Barber, K., Sher, A., Wack, A., & O'Garra, A. (2015). Type I interferons in infectious disease. *Nature reviews. Immunology*, 15(2), 87–103. <https://doi.org/10.1038/nri3787>
- Naqvi, A., Fatima, K., Mohammad, T., Fatima, U., Singh, I. K., Singh, A., Atif, S. M., Hariprasad, G., Hasan, G. M., & Hassan, M. I. (2020). Insights into SARS-CoV-2 genome, structure, evolution, pathogenesis and therapies: Structural genomics approach. *Biochimica et biophysica acta. Molecular basis of disease*, 1866(10), 165878. <https://doi.org/10.1016/j.bbadis.2020.165878>
- Pradhan, V. D., Khadilkar, P. V., Nadkar, M. Y., Kini, S. H., Roumenina, L. T., Rajadhyaksha, A. G., Khan, T. A., Chougule, D., Ghosh, K., Bayry, J., & Kaveri, S. (2021). Impact of Autoantibodies to Complement Components on the Disease Activity in SLE. *The Journal of the Association of Physicians of India*, 69(4), 11–12.
- Röltgen, K., & Boyd, S. D. (2021). Antibody and B cell responses to SARS-CoV-2 infection and vaccination. *Cell host & microbe*, 29(7), 1063–1075. <https://doi.org/10.1016/j.chom.2021.06.009>

- Satarker, S., & Nampoothiri, M. (2020). Structural Proteins in Severe Acute Respiratory Syndrome Coronavirus-2. *Archives of medical research*, 51(6), 482–491. <https://doi.org/10.1016/j.arcmed.2020.05.012>
- Secchi, M., Bazzigaluppi, E., Brigatti, C., Marzinotto, I., Tresoldi, C., Rovere-Querini, P., Poli, A., Castagna, A., Scarlatti, G., Zangrillo, A., Ciceri, F., Piemonti, L., & Lampasona, V. (2020). COVID-19 survival associates with the immunoglobulin response to the SARS-CoV-2 spike receptor binding domain. *The Journal of clinical investigation*, 130(12), 6366–6378. <https://doi.org/10.1172/JCI142804>
- Shcherbak, S. G., Anisenkova, A. Y., Mosenko, S. V., Glotov, O. S., Chernov, A. N., Apalko, S. V., Urazov, S. P., Garbuzov, E. Y., Khabotnikov, D. N., Klitsenko, O. A., Minina, E. M., & Asaulenko, Z. P. (2021). Basic Predictive Risk Factors for Cytokine Storms in COVID-19 Patients. *Frontiers in immunology*, 12, 745515. <https://doi.org/10.3389/fimmu.2021.745515>
- Shrock, E., Fujimura, E., Kula, T., Timms, R. T., Lee, I. H., Leng, Y., Robinson, M. L., Sie, B. M., Li, M. Z., Chen, Y., Logue, J., Zuiani, A., McCulloch, D., Lelis, F., Henson, S., Monaco, D. R., Travers, M., Habibi, S., Clarke, W. A., Caturegli, P., ... Elledge, S. J. (2020). Viral epitope profiling of COVID-19 patients reveals cross-reactivity and correlates of severity. *Science (New York, N.Y.)*, 370(6520), eabd4250. <https://doi.org/10.1126/science.abd4250>
- Squeglia, F., Romano, M., Ruggiero, A., Maga, G., & Berisio, R. (2020). Host DDX Helicases as Possible SARS-CoV-2 Proviral Factors: A Structural Overview of Their Hijacking Through Multiple Viral Proteins. *Frontiers in chemistry*, 8, 602162. <https://doi.org/10.3389/fchem.2020.602162>
- Stoermer, K. A., & Morrison, T. E. (2011). Complement and viral pathogenesis. *Virology*, 411(2), 362–373. <https://doi.org/10.1016/j.virol.2010.12.045>
- Stokes, E. K., Zambrano, L. D., Anderson, K. N., Marder, E. P., Raz, K. M., El Burai Felix, S., Tie, Y., & Fullerton, K. E. (2020). Coronavirus Disease 2019 Case Surveillance - United States, January 22-May 30, 2020. *MMWR. Morbidity and mortality weekly report*, 69(24), 759–765. <https://doi.org/10.15585/mmwr.mm6924e2>
- Sudre, C. H., Murray, B., Varsavsky, T., Graham, M. S., Penfold, R. S., Bowyer, R. C., Pujol, J. C., Klaser, K., Antonelli, M., Canas, L. S., Molteni, E., Modat, M., Jorge Cardoso, M., May, A., Ganesh, S., Davies, R., Nguyen, L. H., Drew, D. A., Astley, C. M., Joshi, A. D., ... Steves, C. J. (2021). Attributes and predictors of long COVID. *Nature medicine*, 27(4), 626–631. <https://doi.org/10.1038/s41591-021-01292-y>
- Trendelenburg M. (2021). Autoantibodies against complement component C1q in systemic lupus erythematosus. *Clinical & translational immunology*, 10(4), e1279. <https://doi.org/10.1002/cti2.1279>

- Uzonyi, B., Szabó, Z., Trojnár, E., Hyvärinen, S., Uray, K., Nielsen, H. H., Erdei, A., Jokiranta, T. S., Prohászka, Z., Illes, Z., & Józsi, M. (2021). Autoantibodies Against the Complement Regulator Factor H in the Serum of Patients With Neuromyelitis Optica Spectrum Disorder. *Frontiers in immunology*, *12*, 660382. <https://doi.org/10.3389/fimmu.2021.660382>
- Vojdani, A., Vojdani, E., & Kharrazian, D. (2021). Reaction of Human Monoclonal Antibodies to SARS-CoV-2 Proteins With Tissue Antigens: Implications for Autoimmune Diseases. *Frontiers in immunology*, *11*, 617089. <https://doi.org/10.3389/fimmu.2020.617089>
- Wallukat, G., Hohberger, B., Wenzel, K., Fürst, J., Schulze-Rothe, S., Wallukat, A., Hönicke, A. S., & Müller, J. (2021). Functional autoantibodies against G-protein coupled receptors in patients with persistent Long-COVID-19 symptoms. *Journal of translational autoimmunity*, *4*, 100100. <https://doi.org/10.1016/j.jtauto.2021.100100>
- Wang, M. Y., Zhao, R., Gao, L. J., Gao, X. F., Wang, D. P., & Cao, J. M. (2020). SARS-CoV-2: Structure, Biology, and Structure-Based Therapeutics Development. *Frontiers in cellular and infection microbiology*, *10*, 587269. <https://doi.org/10.3389/fcimb.2020.587269>
- Wang, E. Y., Mao, T., Klein, J., Dai, Y., Huck, J. D., Liu, F., Zheng, N. S., Zhou, T., Israelow, B., Wong, P., Lucas, C., Silva, J., Oh, J. E., Song, E., Perotti, E. S., Fischer, S., Campbell, M., Fournier, J. B., Wyllie, A. L., Vogels, C., ... Ring, A. M. (2021). Diverse Functional Autoantibodies in Patients with COVID-19. *medRxiv : the preprint server for health sciences*, 2020.12.10.20247205. <https://doi.org/10.1101/2020.12.10.20247205>
- Welberry, C., Macdonald, I., McElveen, J., Parsy-Kowalska, C., Allen, J., Healey, G., Irving, W., Murray, A., & Chapman, C. (2020). Tumor-associated autoantibodies in combination with alpha-fetoprotein for detection of early stage hepatocellular carcinoma. *PloS one*, *15*(5), e0232247. <https://doi.org/10.1371/journal.pone.0232247>
- Wiersinga, W. J., Rhodes, A., Cheng, A. C., Peacock, S. J., & Prescott, H. C. (2020). Pathophysiology, Transmission, Diagnosis, and Treatment of Coronavirus Disease 2019 (COVID-19): A Review. *JAMA*, *324*(8), 782–793. <https://doi.org/10.1001/jama.2020.12839>
- Xiaojie, S., Yu, L., Lei, Y., Guang, Y., & Min, Q. (2020). Neutralizing antibodies targeting SARS-CoV-2 spike protein. *Stem cell research*, *50*, 102125. Advance online publication. <https://doi.org/10.1016/j.scr.2020.102125>
- Disease Outbreak News*. (2020). WHO. <https://www.who.int/emergencies/diseaseoutbreaknews/item/2020-DON229>
[Accessed](#) 05.04.2022.

Clinical Spectrum - COVID-19 Treatment Guidelines. (2022). NIH.

<https://www.covid19treatmentguidelines.nih.gov/overview/clinical-spectrum/>

Accessed 10.06.2022.

WHO Coronavirus (COVID-19) Dashboard. (2022). WHO.

<https://covid19.who.int/>

Accessed 22.07.2022.

8. *Curriculum vitae*

I was born on October 17th 1996 in Zagreb, Croatia. In 2015, I enrolled in the Undergraduate program of Molecular biology at the Faculty of Science, University of Zagreb. In 2017, I had laboratory skill training at Ruđer Bošković Institute in the Laboratory for Cell Biology and Signaling under the supervision of Andreja Ambriović Ristov, PhD. In 2018, I obtained the title of bacc. biol. mol. (*cum laude*) and enrolled in the Molecular biology master's program at the University of Zagreb. In the academic year 2019, I did laboratory practice at Ruđer Bošković Institute in the Laboratory for mitochondrial bioenergetics and diabetes under the supervision of Iva Škrinjar, PhD and Sandra Sobočanec, PhD as a part of SuMERA project. In the winter semester of 2019/2020, I took part in the Erasmus+ exchange and studied in the Regenerative Biology and Medicine master program at Centre for Regenerative Therapies, TU Dresden, Germany. During the winter semester of the academic year 2020/2021, I worked as a quality assurance assistant at Teva Pharmaceuticals in Zagreb. In the summer semester of 2021, I pursued an Erasmus+ traineeship at CRTD, TU Dresden in the Laboratory for Preclinical Approaches to Stem Cell Therapy/ Diabetes where I also worked on my thesis under the supervision of Prof. Ezio Bonifacio, PhD and Anne Eugster, PhD. Later on in 2021/2022, I continued working in the same laboratory as a technical assistant working on different antibody projects. Throughout my studies, I participated in the science popularization event “Night of biology” at my home university. I was a winner of the national STEM scholarship (2017/2018).

9. Supplement



Supplement 1. Schematic of the cloned coding DNA sequences of the antigens of interest fused to the signal peptide IL6 (SP-IL6) and nanoluciferase (NLuc): DDX helicase proteins DDX3X and DDX58 (in green), proteins of the complement system C2, C1r, C1s, CFB, and CFD (in yellow), and SARS-CoV-2 non-structural proteins NSP5 and NSP13 (in grey). The size of the SP-IL6, NLuc, and antigens is not represented in true ratio. Created in PowerPoint.